12-2003

Evidence for an abrupt latest Miocene-earliest Pliocene climate shift preserved in a sinkhole paleolake at the Gray Fossil Site, northeastern Tennessee (Washington County)

Aaron Jacob Shunk

To the Graduate Council:

I am submitting herewith a thesis written by Aaron Jacob Shunk entitled "Evidence for an abrupt latest Miocene-earliest Pliocene climate shift preserved in a sinkhole paleolake at the Gray Fossil Site, northeastern Tennessee (Washington County)." I have examined the final electronic copy of this thesis for form and content and recommend that it be accepted in partial fulfillment of the requirements for the degree of Master of Science, with a major in Geology.

Steven G. Driese, Major Professor

We have read this thesis and recommend its acceptance:

Accepted for the Council:
Carolyn R. Hodges

Vice Provost and Dean of the Graduate School

(Original signatures are on file with official student records.)

To the Graduate Council:

I am submitting herewith a thesis written by Aaron Jacob Shunk entitled "Evidence for an abrupt latest Miocene-earliest Pliocene climate shift preserved in a sinkhole paleolake at the Gray Fossil Site, northeastern Tennessee (Washington County)." I have examined the final paper copy of this thesis for form and content and recommend that it be accepted in partial fulfillment of the requirements for the degree of Master of Science, with a major Geology.

Steven G. Driese, Major Professor

We have read this thesis and
recommend its acceptance:

G. Michael Clark

Claudia I. Mora

Marie E. Uhle

Acceptance for the Council:

Vice Provost and Dean of
Graduate Studies

Evidence for an abrupt latest Miocene-earliest Pliocene climate shift preserved in a sinkhole paleolake at the Gray Fossil Site, northeastern Tennessee (Washington County).

A Thesis
Presented for the
Master of Science
Degree
The University of Tennessee, Knoxville

Aaron Jacob Shunk
December 2003

Dedication

This thesis is dedicated to all those that supported me and encouraged me over the past three years.

Acknowledgments

I wish to thank all that helped me in completing the M.S. in Geology. I would like to thank the Department for the additional financial support for coring. I would like to thank Steve, Maria, Claudia, and Mike (my committee) again for all of their influence- there is no way I could have done this without them. I would like to thank Dr. McKinney, Dr. Wallace, Larry Bristol (my field partner), Martin Kohl, Dr. Parmalee, Dr. Perfect, Dr. H. Delcourt, Dr. P. Delcourt, Dr. Horn, and everyone else that I bothered with a random question from time to time.

Abstract

Records of Neogene terrestrial climate are rare for the eastern half of North America. The recently discovered Gray Fossil Site (GFS) in northeastern Tennessee (Washington County) appears to be a sinkhole paleolake that preserves such a record. Well-preserved vertebrate GFS fossils strongly suggest a Late Miocene–Early Pliocene (Hemphillian) Land Mammal Age ($\geq$ 4.5 Ma). Three distinct facies occur within the upper 20 m of GFS lacustrine sediment. The *graded facies* is characterized by continuous succession of individual graded beds that average 0.8 cm thick. This facies contains < 1% total organic carbon (TOC), has carbon isotope composition (δ^{13}C V-PDB) averaging –25.4‰ with values as positive as –24.3‰, and is interpreted to represent deposition from sporadic storm events in a water-stressed ecosystem. The *laminated facies* overlies the *graded facies*. The transition between the two facies is marked by: 1) the development of a depositional pattern that grades into the laminated facies, 2) an abrupt increase from <1 % to ~ 9 % TOC, and 3) the steady decrease of δ^{13} C values to those typical of the *laminated facies*. The *laminated facies* consists of laterally continuous sediment couplets that average 0.4-0.6 cm thick and consist of a thin, coarse-grained, and organic-rich terrigenous (A) lamina added to the apparently continuous deposition of silty-clay terrigenous matrix that comprises the (B) lamina. The couplets contain statistically significant 5-couplet periodicity; the couplets are therefore interpreted to be annual varves with variable thickness possibly related to ENSO cycles. The *laminated facies* averages ~ 8 % TOC with δ^{13} C values that average –29.3‰, and is interpreted to represent a wetter overall climate with a distinct high-energy wet season. Using the varve couplets at the base of the *laminated facies* to establish a sedimentation rate (which likely underestimates the sedimentation rate at the top of the graded facies), the majority of the facies change appears to have been deposited in less than 500 years. A *subaerial facies* records soil formation and filling of the sinkhole lake.

The possible shift from a drier climate to a wetter, seasonal climate documented in the changing paleolake sediment facies at the GFS may have been caused by a eustatic sea level rise documented at ~ 5 Ma. Sea level rise is proposed to have caused a brief period of upwelling along the Atlantic coast of North Carolina.

TABLE OF CONTENTS

LIST OF TABLES

LIST OF FIGURES

1. INTRODUCTION:

The Late Miocene to Early Pliocene was a transitional time in Earth history. During the Late Miocene (8 to 6 Ma) there was a global increase in C_4 grassland ecosystems, which expanded into middle and high latitudes (Cerling et. al., 1997); this change was accompanied by the most significant Cenozoic faunal turnover (Cerling et al., 1998). Ungulate survivorship patterns from the Late Miocene extinction indicate that the North American climate underwent some combination of cooling, drying, and an increase in the seasonality of temperature and/ or precipitation during the Late Miocene (Janis, 1989). *Gomphotherium* tusk growth patterns also indicate that seasonality increased in parts of North America during the Late Miocene and Early Pliocene and suggest that the onset of seasonality is attributable to an increase in aridity and precipitation (Fox, 2000). Starting at 4.6 Ma the shallowing of the Central American Isthmus caused the Atlantic Ocean circulation pattern to be reorganized, whereby the Gulf Stream intensified and North Atlantic Deep Water developed (Haug and Tiedemann, 1998). From about 5 to 4 Ma, a marine transgression caused oceanic waters to move onto the Atlantic continental margin adjacent to North Carolina, and the early stages of this transgression were characterized by phosphate sedimentation that resulted from the upwelling of cold, nutrient-rich deep waters into the local embayment (Riggs and Belknap, 1988). From 3.1 to 2.5 Ma, Northern Hemisphere glaciation intensified in response to the increase in atmospheric moisture resulting from the alteration to the Atlantic Ocean circulation pattern and changes in the Earth's orbital obliquity (Haug and Tiedemann, 1998).

Today, the Gulf Stream supplies warm, equatorial surface water to the Atlantic coast of North America. Prior to the establishment of the Gulf Stream, the presence of cold surface waters along the Atlantic coast could have profoundly affected terrestrial climate, the amount of moisture, and the terrestrial fauna. Unfortunately, there is little information available about the terrestrial climate of the eastern half of North America from this important transitional period in Earth history. The recently discovered Gray Fossil Site (GFS) is an unusual geological setting that contains a continuous record of lacustrine sedimentation spanning the Late Hemphillian (latest Miocene-earliest Pliocene). The GFS is located in East Tennessee (36.5°N, 82.5°W); only one other Tertiary biota from the interior of North America is known to exist east of the Mississippi River. The Pipe Creek Sinkhole Biota is an Early Pliocene site located in northern Indiana and, based on the fauna and flora preserved within the site, the paleoenvironment of northern Indiana has been interpreted as dry, open and perhaps prairie-like, but with trees nearby in the Early Pliocene (Farlow et al., 2001).

In this thesis, I present research with two primary objectives, namely: 1) to reconstruct the paleoenvironment and paleoclimate of the latest Miocene-earliest Pliocene aged GFS using field stratigraphic relationships, petrographic analysis, organic matter stable isotope compositions, and time series analysis, and; 2) to attempt to evaluate the observations from the GFS in a regional perspective, in particular, the possible response of climate to the concurrent reorganization of the Atlantic Ocean.

2. SITE DESCRIPTION:

The Gray Fossil Site (GFS) was discovered in May of 2000 when heavy machinery working to extend a local highway in eastern Tennessee cut into dark colored, unlithified sediments (Fig. 1). The elliptical site extends laterally about 2.6 ha (150 m north to south by 175 m east to west) and is filled with what is apparently a continuous 40 m record of dominantly silty-clay lacustrine sediment deposited during the Late Tertiary, based on the fossil assemblages. The lateral extent of the deep, lacustrine sediments is about 1.6 ha. The sediments contain abundant Knox Group (Cambro-Ordovician) dolostone boulders that can exceed 4 m in diameter, as well as multiple graded layers composed primarily of 1 to 10 cm diameter clasts of Knox dolostone and chert (Figs. 2 and 3). A diverse terrestrial and aquatic vertebrate fauna and flora are also preserved within the GFS sediments.

The GFS is located on a fold limb underlain by dolostone of the Knox Group (Cambrian-Ordovician), a stratigraphic unit in which deep, near-vertical solution features commonly form, with patterns of cavity development that mimic structural features, such as faults and fold limbs (Redwine, 1999). This ancient, deep lacustrine paleoenvironment contains at least three distinct facies. From the top downward, these include: (1) A *subaerial facies,* ~ 10 m of sediment colluvium and alluvium regolith overlying paleosols that formed from the underlying lacustrine sediments (Fig. 4) (Clark, pers. comm., 2002; Driese, pers. comm., 2002; Smith, M.S. thesis in progress). An unconformity of unknown duration separates the upper paleosol from the regolith. (2) A distinctly-laminated lacustrine facies (hereafter referred to as the *laminated facies*) characterized by dark-light colored couplets that average ~ 4-6 mm thick. Each couplet consists of an organic-rich, dark brown to black colored (A) lamina that alternates with a silty-clay, gray colored (B) lamina. More than a $40m^2$ area of the distinctly laminated lacustrine facies was exposed by road construction, and the laminations are laterally continuous where exposed (Fig. 3). (3) The graded lacustrine facies (hereafter referred to as the *graded facies*) dominantly consists of individual 0.1 to 2 cm thick beds composed of fine sands that grade upward into silt and clay. This facies appears cryptically laminated due to color differences between the coarse and fine components of the individual beds and appears to be exposed along the southwestern edge of the GFS. The dimensions of the deep lacustrine sediments (~1.6ha by 40m), the location of the site within the Knox Group dolostone on a fold limb, and overall stratigraphy are evidence that the GFS represents an ancient, elliptically-shaped 40m deep-sinkhole lake that formed from a solution (karst) feature within the local Knox Group bedrock.

The presence of a paleomagnetic reversal within the upper lacustrine sediments (Clark, pers. comm., 2001) provides a minimum age of 0.78 Ma for the GFS (Cande and Kent, 1995). The occurrence of *Tapirus*, cf. *T. polkensis*, *Teleoceras* sp., a small *Megalonyx* sp. or *Plimetanastes* sp., and cf. *Catagonus* sp. within the laminated facies strongly indicate that the mammals belong to the Hemphillian Land Mammal Age and date to the Late Miocene-Early Pliocene ($\geq$ 4.5 Ma) (Parmalee et al., 2002). The only other available date for the site is derived from *Teleoceras* sp., which developed carpal variability throughout its existence (Harrison and Manning, 1983). The presence of medial projections on the posterior processes of the rhinoceros's unciforms suggests a late Hemphillian (4.5-5.5 Ma) age for the GFS, because this feature is only common at the end of the *Teleoceras* lineage in the latest Miocene to earliest Pliocene (Manning, 2003). During the late Hemphillian magnetic polarity was reversed from 5.230 to 5.894 Ma, and also at adjacent intervals of time before (6.137-6.269 Ma) and after (4.890-4.980 Ma) the late Hemphillian (Cande and Kent, 1995). Because the GFS occurs within a region where late Tertiary biotas are rare, it is possible that timing of the evolution of *Teleoceras* sp. carpal features varied or that the extinction of the rhinoceros was delayed. Therefore, the latest Miocene to earliest Pliocene date for the GFS should be accepted with some caution.

The incredible state of preservation of both the organic matter and the vertebrate fossils indicates that little destructive diagenesis has occurred throughout the history of the site (Fig. 5). Included within the GFS fauna are multiple fossil crocodilians that constrain paleoclimate conditions. Temperature is the principal influence on the global distribution of crocodilians, and a Coldest Month Mean temperature (CMMT) of > 5.5°C is the minimum thermal limit for the group (Markwick, 1998). The presence of crocodilians within the GFS *laminated facies* suggests that the site did not freeze annually.

3. METHODS:

I. SAMPLING:

Samples for petrographic, isotopic, and spectral analysis were collected from a combination of field localities and cores. Because the GFS was discovered by heavy machinery extending a local road, there is the equivalent of two overlapping road cuts trending northwest-southeast through the upper, central portion of the GFS sediments (Fig. 1). Various field samples were collected from the sediments exposed by construction crews. Sediments from field cut 1 extend from about 505 to 504 m above sea level and include the transition from the subaerial facies to the distinctly laminated lacustrine facies. Cut 2 is about 6 m southwest of cut 1 and contains sediments extending from about 503.7 to 501.6 m above sea level, and there is a small covered interval between the two cuts.

About 15 m of 3 cm diameter core were collected from the deepest portion of the site, using a push core rig. Core 1 was sampled about 25 m southeast of cut 2 (Fig. 2). Core one was refused at 8.2 m and a section of core spanning 3.14 to 4.36 m was lost. At refusal, the rig was moved about 3 meters west of core 1 and core 2 was taken. The rig augured down to 3.5 m and retrieved a representative section overlapping with the lost section, and then resumed coring from 8.5 m to 14.76 m. The nearly continuous 14.76 m of core was stored in a freezer at -5°C until processed, and half of the core remains archived at the University of Tennessee.

II. PETROGRAPHIC ANALYSIS:

Samples for thin-section analysis were collected at 13 representative elevations within the GFS stratigraphy (Fig. 6). Samples 1 through 7 were taken from cut 1 and cut 2, within the lacustrine sediments, and samples 7 to 12 were taken from core 1 and core 2. Sample 0 was retrieved from the uppermost sediments from the center of the site. Samples were completely dried under a vacuum hood and then coated with resin prior to commercial thin-section preparation.

III. SEDIMENT ACCUMULATION:

Sediment accumulation research was conducted using a 1.3 m long by 6.6 cm wide glass settling-column that was placed upright so as to remain perpendicular to the ground (Fig. 7). The settling-column was filled with distilled water and about 5 cm of powdered $CaCO_3$ was allowed to completely settle to the bottom of the cylinder in order to make a high contrast, dense and flat bottom layer. Four, 5 g samples of sediment from the *laminated facies* were collected and placed

into a beaker containing 40 mL of distilled water. These samples were taken from the most distinctly laminated sediments within the laminated facies (Fig. 8). The beaker was shaken lightly until the sediment became fully suspended within the fluid. The water and suspended sediment were then poured into the vertical tube and allowed to settle through the pure water for a distance of 1 m.

Sediment accumulation data were collected using 10x magnification glasses to measure the thickness of the sediment as it settled onto the bottom. Thickness data were collected at intervals of about 10, 30, 45, and 60 seconds, and then at every minute thereafter up to 30 minutes. After 30 minutes, data were collected at 35, 45, 50 and 60 minutes, and then at 2 hours, and finally at 24 hours. Four individual experiments were conducted and samples were allowed to completely settle for at least two days between experiments. Data were measured from the high-contrast contact between the carbonate powder and the top of the settled portion of the sediment. Data were measured in mm, with one interpolated decimal point.

IV. STABLE ISOTOPES AND ESTIMATION OF %TOC:

Thirty-three samples were collected from the GFS sediment for stable carbon isotopic analysis and determination of approximate weight. Six organic (A) laminae and 6 silty-clay (B) laminae, as well as one bulk sample, were separated from the most distinctly laminated sediments (Fig. 8, Table 2). Samples were collected from the *subaerial facies*, the *laminated facies*, and the *graded facies* (Fig. 6, Table 1).

Isotope ratios were measured using a Finnegan MAT Delta ^{plus} mass spectrometer. Research samples were prepared by treating powdered bulk sediment with 10% HCl for 1.5 hours to remove the carbonate portion of the samples. About 0.1g of sample was loaded into a sealed glass tube with 0.5g Cu, 0.5g CuO, and a small piece of Pt wire and combusted at 1000°C for four hours. CO_2 was collected on a vacuum line, cryogenically purified, and analyzed isotopically in the spectrometer. δ^{13} C results are reported in the standard per mil (‰) notation relative to the V-PDB standard. The value of the USGS-24 standard was -15.918 ± 0.011‰(n=4).

Estimated %TOC values were derived during the CO_2 collection process for isotopic analysis. A manometer on the vacuum line quantifies the amount of CO_2 created during the combustion of each sample. The % TOC can be derived from the amount of CO_2 released, but this value is subject to modest errors introduced during the weighing and loading of samples. The analytical precision of the estimated %TOC has not yet been determined.

V. TIME SERIES ANALYSIS:

The data for time series analysis were collected in the field from carefully constructed trenches that were cut perpendicular to the laminated bedding within field cuts 1 and 2. Data were collected manually using 10x magnification glasses to place a very thin needle into the center of a sequence of organic (B) laminae. The distance between the needles, as well as the laminae thicknesses, were measured with a metric ruler and recorded as a continuous sequence in millimeters, with one additional interpolated decimal point (Table 3). A total of three data sets were collected from cut 1 and cut 2, but two were not continuous due to the presence of disrupted sections of sediment within the sequence. Data set two consisted of 98 continuous data points from cut 2 and was therefore used for spectral analyses.

The data were recorded as a continuous sequence of laminae thickness, and evaluated using the Proc Spectra procedure in the SAS-ETS program in which the x input was the distance between adjacent points and the y input was the data rank. Spectral analysis of the series was performed with the weights statement, weights 1 2 3 4 3 2 1. This statement specifies a triangular spectral window (kernel) to smooth the periodogram in order to reduce the random component and produce a spectral density estimate. From this estimate, a periodogram was constructed to express the variances of the successive harmonics from the data set by plotting period against the spectral density function.

A periodogram must be coupled with statistical evaluation of the data to determine if it represents white noise. Proc Spectra produces two statistical tests, Fisher's Kappa (Davis, 1941; Fuller 1976) and Bartlett's Kolmogorov-Smirnov statistic (Fuller, 1976; Durbin 1967), to determine if the largest periodogram ordinate can be considered significant from white noise. With a data set of 97 points Fisher's Kappa must exceed a critical value of 7.34 (Fuller, 1976) and the Bartlett's Kolmogorov-Smirnov statistic must exceed 0.1459 (Owen, 1962) to surpass the 95% confidence interval and be considered significant from white noise.

4. **RESULTS:**

I. PETROGRAPHIC ANALYSIS:

Analysis of 14 oriented thin-sections prepared from field samples and cores verified that three distinct facies exist within the upper 10 m of GFS sediment (Fig. 6). In the field the *graded facies* is differentiated by its light gray color (Munsell color 2.5 Y/5/1 to 2.5 Y/4/2) and reduced amount of visible organic matter. Petrographic analysis revealed that the *graded facies* occurs between an elevation of 491 m to about 496 m (although it occurs in sediments as deep as 486 m elevation). The *graded facies* is characterized by the long intervals (>1m) of a continuous succession of graded beds that average 0.8 cm thickness. The thick graded beds normally size-grade from fine to medium sand to clay (Fig. 9). The facies consists of sub-rounded to rounded quartz and dolostone clasts that typically grade into finer particle sizes with predominantly the same composition. Quartz grains with volcanic resorption rims and embayments exist within the graded beds that are derived from 80 km away to the southeast in Virginia (Smith, 2003). The contacts between adjacent beds can be sharp (Fig. 9a), or the deposition of the fine silt and clay component can be interrupted by the deposition of the coarse component of a new bed (Fig. 9e). Siderite and pyrite are present throughout the *graded facies* and occur as graded clasts or as individual layers between graded beds.

The thickness of individual graded beds ranges from between 0.1 cm to >1 cm, and the total thickness of a bed is related to the thickness and the maximum grain size of the sand fraction at the base of the bed; coarser grain sizes and a thicker coarse component correlate with thicker total beds. Petrographic analysis revealed that two distinct depositional patterns exist within the graded facies. The first depositional pattern consists of sequences of relatively thick individual graded beds that can persist for intervals >1 m (Figs. 9a and 9d). The second depositional pattern is characterized by a sequence of sediments that contain mixed silt and clay matrix and very thin, intermittently deposited (<0.3 cm) graded beds (Figs. 9c and 9g). Within the *graded facies,* the distribution of thin/mixed bed depositional pattern and the thick bed depositional pattern is not random because the sediments are deposited in discrete sequences that are exclusively composed of either the thin or the thick graded beds (Fig. 9b). The thin/mixed depositional pattern intermittently interrupts the intervals of graded beds in a rhythmic pattern, and the frequency of the thin/mixed depositional pattern becomes more prominent up-section within the *graded facies* until the couplets that characterized the *laminated facies* develop from the consolidation of the ever-thinning sequences of graded beds and mixed non-graded sub-layers (Fig. 6).

In the field, the *laminated facies* is differentiated by its dark color (Munsell color 2.5/1/N to 2.5 Y/3/3) and the presence of couplets that alternate between coarse organic- rich laminae and silty clay laminae. Petrographic analysis revealed that the dark-colored (A) laminae consist of organic layers that are dominantly composed of terrestrially derived plant debris and contain abundant large quartz, dolostone, and rip-up paleosol grains that are uncommon within the (B) laminae (Fig. 8). The (B) laminae are primarily composed of a silty-clay matrix with birefringence that goes extinct parallel to bedding. The silty-clay matrix consists of fine carbonate (dolomite) rock flour and clay mixed with silt-sized quartz and dolostone clasts. Neither the (A) nor (B) laminae are graded within the upper portion of the series of laminated sediments.

Couplets at the base of the *laminated facies* (at an elevation of about 501 m) are characterized by variable thicknesses, and the thickness of the individual couplets can exceed 3 cm; however, the average couplet thickness is 0.71 cm. Within this zone (Fig. 10c), couplets regularly break apart and the organic (A) laminae become interrupted by intermittent silty-clay matrix sub layers. Continuing up-section (to an elevation of ~ 502.5 m) the laminations become more regular and the thickness of individual couplets varies in a distinct cycle, in which the thickness of couplets oscillate between thin (0.2 - 0.6 cm) and thick (1.2 -1.6 cm) intervals over a period of about 25 couplets (Fig. 11). Further up-section (at an elevation of about 504.5 m) the couplets within the *laminated facies* continue to thin and have an average thickness of 0.5 cm. The most distinctly laminated sediments observed from the GFS came from the upper most, central portion of the site that was destroyed by excavation for road construction. These sediments couplets have an average thickness of 0.39 cm and consist of distinct dark brown to black (A) laminae that alternate with light brown (B) laminae (Fig. 12d). The (A) laminae average 1 mm thick, whereas the (B) laminae average 2.9 mm thick.

The *laminated facies* consists of a combination of local and extrabasinal clasts (Fig. 13). Locally-derived clasts include angular Knox Group dolostone grains (Fig. 13e) that vary in size from silt to pebbles, and reworked soil aggregates (rip-up clasts) derived from laterally adjacent paleosols (Fig. 13a). Exotic clasts include metaquartzite clasts (Fig. 13c), which are derived from > 20 km to the northeast in the Blue Ridge, and volcanic quartz clasts with resorption rims and embayments that are derived from 80 km away to the southeast in Virginia (Fig. 13b) (Smith, 2003). The *laminated facies* also contains precipitated grains of gypsum rosettes, pyrite, iron and manganese oxides, and siderite, but these grains are minor compared to the terrestrially derived clasts.

Most of the transition from the *graded facies* to the overlying *laminated facies* occurs between ~ 497 and 500.5 m elevation. The thin/mixed depositional pattern within the *graded facies* gradually grades into the couplets that characterized the *laminated facies*, and although the transition is complex, it can be generally qualified into a temporal sequence of events (Figs. 6, 10). These events are: 1) At an elevation of about 496.5 m short (~ 5 cm) intervals of the thin/mixed depositional pattern develop and intermittently interrupt the continuous succession of individual thick graded beds, 2) the thin/mixed depositional pattern occurs more frequently until it dominates the stratigraphy, 3) the thin-graded beds and the mixed non-graded layers begin to cluster and the depositional pattern becomes chaotic, 4) the amount of organic matter increases and the coarse-grained (A) laminae develop but remain irregular, and 5) by an elevation of 501. 5 m, thick (average 0.71 cm) couplets with distinct (A) and (B) laminae have developed.

The thin/mixed depositional pattern and the thick graded bed depositional pattern occur as discrete entities (Fig. 9b). The thin/mixed depositional pattern is characterized by thin graded beds that have an average thickness of about 0.1 to 0.3 cm (Figs. 9f, 9g); within the thin/mixed intervals there are many layers of mixed, non-graded sediment that average from 0.2 to 0.3 cm thick. The development of the thin/mixed depositional pattern occurs intermittently (Figs. 6, 10). Below an elevation of about 496 m the sediments are dominantly composed of individual graded beds that average about 0.8cm thick (Fig 9a). At an elevation of about 497 m the sequences of thin/mixed deposition begin to sporadically interrupt the thick graded bed depositional pattern, and by an elevation > 500 m the thin sequences dominate the depositional pattern (Fig. 9c), and the average thickness of individual beds has decreased to about 0.2 cm. At an elevation of about 496 m nominal amounts of mixed sediment occur within the large graded beds. At an elevation of about 498.5 m mixed sediments encompass an estimated 20% of the sequence and the graded beds comprise the remaining 80%, but by an elevation of about 500.2 m mixed sediments comprise about 60% and the graded beds are about 40% of the total sequence.

The base of the *subaerial facies* consists of a paleosol that developed upon subaerial exposure of the laminated facies and it is differentiated in the field by its red to orange color (Munsell color 10 YR/6/8 to10 YR/4/6). The *subaerial* and *laminated facies* contact abruptly grades from the distinctly laminated lacustrine parent material to an oxidized soil B-horizon that has seen removal of the carbonate and organic component of the lacustrine parent material (Fig. 14f). In the field, this transition is made apparent by a distinct color change where the Munsell color of 10 YR/6/8 to10 YR/4/6 of the B-horizon changes to the typical 2.5Y/5/1 to 2.5Y/6/1 range of color for the laminated lacustrine sediments over an interval of 3 cm (Fig. 4). The

paleosol has a coarse blocky ped structure and abundant pedogenic features including: a reoriented clay matrix, iron oxide, manganese, and root traces and burrows with illuviated clay deposits (Fig. 14). These features are consistent with a paleoAlfisol. The paleoAlfisol occurs from ~ 504.7 to 505.2 m elevation before giving way to another paleosol that is characterized by a mottled gray component mixed within red orange sediments (Munsell color 10 YR/5/8 and 8/5/PB). The mottled paleosol appears to be the same as a paleoVertisol with diagnostic slickensides discovered nearby within the GFS basin (Smith, 2003). The paleoVertisol contains reworked sections of laminated lacustrine sediments that are very similar to the *laminated facies* (Driese pers. comm., 2002). The mottled paleosol exists at an elevation of ~ 505.2 to 506 m before giving way to the chert-rich Knox residuum cover mass. The cover mass persists to the top of the GFS deposit at an elevation of 507.2 m and consists of coluvium and alluvium sediments (Clark pers. comm., 2001; Smith, 2003). Illuviated clays from pedogenesis (possibly modern) are observed to fill cracks as deep as 8 m into the GFS lacustrine sediments, and root traces exist within the upper sediments of the *laminated facies.*

II. SEDIMENT ACCUMULATION:

Results of settling experiment are shown in Figures 15-16. The sediment from the GFS laminated facies settled through the 1 m settling column in a consistent pattern; i.e., in all four experiments the sediments settled in two distinct suites based on particle size. The coarse suite consisted of fine to coarse sand particle sizes and large disk-shaped pieces of organic matter. The fine suite of sediment consisted of the silt and clay components of the sediment. Organic clasts were the first to settle and thus had the highest settling velocity. The organic component dominantly consisted of dark colored, disk to sub-angular shaped pieces of organic matter that were about 0.5mm to 2mm in diameter. Under a microscope, the organic clasts had a vascular structure that indicates they are derived from terrestrial land plants. Quartz and carbonate sand-sized clasts were the next to settle. The organic and quartz sand components completely settled out of the water within the first two minutes. From 2 to 6 minutes very little sediment was deposited on the bottom, and this hiatus separated the coarse suite from the fine suite of sediment in all four experiments.

At about 8 minutes, the silt and clay component of the sediment began to accumulate on the bottom, and it took about an hour and a half for the majority of the silt and clay component to reach the bottom of the settling column. The settling velocity of the *laminated facies* sediment was a function of particle size. The entire coarse fraction settled at a rate of >1m/ min (Fig. 16),

and some individual large organic grains had settling velocities > 1m/ 5 seconds. By contrast, the individual clay flocculants took on average 15.4 minutes to settle through the 1m vertical distance of the column (Fig. 17).

Once the entire sediment load from the 4 experiments was deposited and had settled, the beds were obviously graded (Fig. 7). The organic constituent of the sediment contacted the fine portion of the previous bed and then was typically size-graded into medium and fine sands, then silt, and finally clay particle sizes. Although the experimental beds seemed to be laminated, the laminations were the result of color changes in the normal grading from organic matter to sand to silt to clay particle sizes. The sediment structure from the experimental beds is in sharp contrast to the original structure of the *laminated facies* sediments, in which neither the (A) laminae nor the (B) laminae are normally graded (Fig. 8b).

The average maximum bed thickness produced from the 5g of GFS *laminated facies* sediment was 3.3 cm thick, and this thickness occurred about one hour after the sediment was inserted into the settling column and before all of the clay particles had been deposited. After two days the average bed thickness decreased to 1.4 cm. The same trend, in which deposited sediments thin with time, was observed within the coarse suite of sediments during the hiatus from 2 to 6 minutes (Fig. 16). For up to 12 hours after the initiation of each experiment, when individual pieces of organic matter were inserted into the settling column they settled to the bottom and penetrated the silt and clay component of the bed. When organic clasts were introduced about 2 hours after the experiment began, they easily penetrated the silt and clay component without leaving a trace, but as time progressed inserted grains left a vertical tube where it penetrated the fine portion of the bed. Eventually each bed consolidated enough to support the influx of new coarse material without significant penetration. When the experimental beds became stable (after two days of consolidation), the coarse component produced a <2.5mm layer that is < 18% of the total experimental bed thickness. In contrast, within the original *laminated facies* sediments from the GFS the organic layers average about 33% of the total laminae thickness.

III. STABLE ISOTOPES AND ESTIMATION OF %TOC:

The δ^{13} C values of samples analyzed from the upper 20 meters of the GFS lacustrine sediments ranged in value from -24.3 to -29.6‰ V-PDB (Fig. 18). The *laminated facies* sediments were the most depleted in ^{13}C and averaged -29.3‰, except where the pedogenic processes (that characterize the *subaerial facies*) occurred and produced oxidized sediments with

enriched isotopic values averaging -26.5‰. Isotopic values from the underlying *graded facies* sediments averaged -25.8‰. When the organic (A) and silty-clay (B) laminae from the distinctly laminated facies were manually separated and analyzed individually there was only a slight variation between laminae, with the organic layers averaging -29‰ and the silty-clay layers averaging -29.5‰ (Fig. 18). Estimated percent total organic carbon values (%TOC) varied considerably within the GFS sediments. The *laminated facies* averaged 8% TOC, except for the samples taken from the paleosol that formed in the laminated lacustrine sediments and from the transition zone between the paleosol and the *laminated facies*, which were 0.2% TOC and 2.2% TOC, respectively. The *graded facies* averaged 0.4% TOC. In cases in which the (A) and (B) laminae were physically separated, the organic (A) laminae averaged 16.4% TOC whereas the silty-clay (B) laminae averaged 6.5% TOC (Fig. 18).

IV. TIME SERIES ANALYSIS:

Time series analysis of 97 continuous couplets within the GFS *laminated facies* produced a Fisher's Kappa test statistic of 7.42 and a Bartlett's Kolmogorov-Smirnov statistic of 0.31, which exceed the 5% (95% confidence) critical values of 7.34 and 0.146, respectively. These values eliminate the null hypothesis that the maximum periodogram ordinate value, at a period of 5 units, is white noise (Fig. 19). Also displayed on the periodogram are interesting peaks at about 7 and 25 units, and although these peaks cannot be considered different than white noise they may reflect quasi-periodic signals from the data set.

5. INTERPRETATION AND DISCUSSION:

I. GFS BASIN CHARACTER:

The GFS appears to represent an ancient sinkhole lake that filled up at some time during the Late Hemphillian (4.5 to 5.5 Ma). Sinkholes originate from the dissolution of the underlying carbonate host rock, and the function of a sinkhole is to transmit surface water underground into the aquifer. Lake development from a sinkhole is through progressive sequential stages to maturity that can be delineated into geomorphic types. Sinkhole lakes in north-central Florida can be divided by geomorphic types into progressive developmental phases that include: 1) the active subsidence or collapse of the sinkhole; 2) the plugging of the sinkhole with sediment; 3) the mature lacustrine environment that accumulates sediment until the basin fills; and 4) subaerial exposure characterized by broad flat bottomed basins that are inundated at high stages of the water table (Kidinger et al., 1996). Although the host rock, structural features, and the drainage of sinkhole lakes in north-central Florida are not equivalent to eastern Tennessee, the conceptual model of sinkhole lake formation and evolution is consistent with the sediment record of the GFS (Fig. 20). Alternatively, the evolution of the GFS basin could have included a period of time when the basin was a closed cave lake environment that received sedimentation exclusively from groundwater discharge. If this were the situation, then the presence of abundant aquatic vertebrate fossils is evidence that the cave eventually opened into a lacustrine environment.

The GFS basin may have received sediment from surface discharge, groundwater discharge, eolian processes, or some combination of these mechanisms at various times throughout its history. Sediment from surface discharge could have been transported by a creek, river, sheet flow, or any combination of these mechanisms. Groundwater discharge could have been filtered thorough small spaces and therefore size sorted or it could have been delivered through large sub-surface conduits that allowed large particles to be transported. Eolian processes can only transport fine particle sizes, but it is possible that they delivered considerable amounts of sediment into the site. The presence of abundant extrabasinal clasts derived from ~ 80km to the northeast (Mt. Rogers area) and clasts derived from > 20km to the southeast (Blue Ridge) (Smith, 2003) suggests that the GFS received sediment from considerable distances to the east. Preliminary core data indicate that the east-facing bank of the GFS had a gentle slope relative to the west bank (Whisner, 2001) that is consistent with denudation associated with surficial water entering the site from the east, and the presence of fluvial quartz clasts within the lacustrine sediments, soil rip-up clasts within the *laminated facies*, and large complete leaves within the upper *graded facies* and *laminated facies* indicates that the site was fed by a creek or

river throughout part of its history. Although there is evidence for fluvial deposition of sediment into the GFS basin, more research is needed to understand the sedimentation processes throughout the sites history. It is possible that the drainage into the GFS included groundwater inputs and/ or considerable eolian sediment, in combination with the surface drainage.

Like all lakes, sinkhole lakes are ephemeral features on landscapes that are characterized by a continual shallowing and regression throughout their history as they fill with sediment. The GFS depositional environment accumulated about 40 m of dominantly clastic lacustrine sediment throughout its depositional history. The uppermost 20 m of sediment appear to be continuous, and the preservation of the original sediment fabric without evidence of bioturbation, and the presence of precipitated pyrite throughout the lacustrine depositional history, suggest that the site maintained poorly oxygenated or anoxic bottom waters throughout its history. The sediment record can be characterized into a vertical sequence in which the *graded facies* gradually grades into the *laminated facies*, which then abruptly grades upwards into the *subaerial facies* (Fig. 6). The facies shift within the GFS lacustrine sediments from a nearly continuous succession of individual graded beds that characterize the *graded facies* to the couplets that characterize the *laminated facies* indicates that significant changes to the depositional pattern of sediment in the GFS changed significantly ~ 4m down-section from the subaerial exposure of the basin. The facies shift within the GFS sediments is somewhat consistent with the idealized vertical succession of a filling lake; as a lacustrine environment fills with sediment throughout its history the grain size and/or amount of organic matter increase near the top of the lacustrine basin (Picard and High, 1981). However, the distinct variation in depositional pattern may indicate that significant changes occurred to the climatic mechanism of sediment delivery into the GFS basin. Therefore, it is necessary to evaluate available data to determine if the facies shift within the GFS stratigraphy relates to: 1) changes within the GFS basin as it matured and filled up, or 2) changes from the climatic forcing of sedimentation, or 3) some combination of factors.

II. SEDIMENTOLOGY

II a. *Graded Facies*

Graded beds have been attributed to individual events of deposition ranging from a storm-generated cloud of suspended sediment (Pedersen, 1985) to turbidity currents (O'Brien, 1996). Anderson and Dean (1988) described a depositional pattern from Coldwater Creek near Mount St. Helens, in Washington, that is partially relevant to the depositional pattern responsible

for producing the individually graded beds within the GFS *graded facies*. In May, 1980 the eruption of Mount St. Helens removed vegetative cover surrounding Coldwater Lake, thus leaving the drainage mantled with highly erodable materials and creating an unusual situation in which the combination of the abundant and seasonally distributed precipitation, and slopes out of equilibrium with soil development and vegetative cover, resulted in very high sediment yield and seasonally deposited turbidites. Sediment trap studies revealed that the first heavy storms at the onset of the wet season mobilized most of the annual load of sediment in a "first flush" that produced silty turbidites. During the remainder of the wet season a mix of silt and clay was deposited, and during the dry season a layer of clay was deposited. If this temporary depositional pattern had continued indefinitely the resulting annual increments of sediments would have had a graded structure similar to glaciolacustrine varves.

The "first flush" model of Anderson and Dean (1988) offers valuable insight about the depositional pattern producing the graded facies, but the sequence of sediments within the *graded facies* is far more complicated then Anderson and Dean's (1988) ideal annual increment of sedimentation. The model shows the important role of vegetative ground cover in regulating the movement of clastic material into lakes, as indicated by the change in depositional pattern associated with the abrupt removal of the vegetation. It also points out the potential for entrainment and deposition of large amounts of sediment during one high-energy event, and the effect that a seasonal climate can have on the depositional pattern. It also indicates the important role that unstable slopes (even if local) could have played in the deposition of the sequence of the GFS sediments. If the GFS formed as a steep-sided sinkhole and evolved into a sinkhole lake with a gently sloping east bank (Fig. 20), then it is likely that during a considerable portion of time that the GFS was accumulating sediment that the local environment had sloped banks that were in geomorphic disequilibrium. If this was the situation then it is likely that most of the sediment eroded from the bank was deposited into the GFS environment. Although no effort was made to determine the volume of sediment removed from the local environment, it is possible that a considerable amount of local sediment was deposited into the GFS during the geomorphic evolution of the basin, and that this additional local sediment could have produced extremely high sedimentation rates during portions of the GFS sedimentological record.

Comparing the "first flush" model with the results of the results of *graded facies* analysis indicates that the elegantly graded beds with rare interruptive bed of the GFS *graded facies* necessitates a different depositional mode. Individual graded beds within the graded facies typically grade from fine sand to clay in a continuous, uninterrupted pattern in which every up-

section portion of the bed is consistently finer than the sediments underneath (Fig. 9d). This degree of grading varies from the expected beds produced from multiple depositional events, of variable energy, suggested by the "first flush" model. Assuming that the depositional environment was constant, the "first flush" depositional pattern would likely generate a single individually graded bed that resulted from the initiation of the seasonal deposition of sediment with a generally fining-upward sequence, with minor perturbations stacked on top that resulted from the remainder of the wet season and the dry season. Most of the graded beds within the *graded facies* are completely graded, which indicates that the individual graded beds formed in response to individual depositional events. Also, within the *graded facies* the deposition of the fine particle component of the individual graded beds is occasionally interrupted by the subsequent deposition of additional coarse sediment that is equivalent, in both particle size and amount, (expressed as thickness in thin-sections) to the coarse component of the previously deposited bed (Fig. 9c). This indicates that in instances when interruptive beds are present, the amount of time required for the fine component of sediment from the first depositional event to settle onto the lake bottom was less than the amount of time between adjoining depositional events. In other words, the interruptive beds formed when the frequency of storms events exceeded the amount of time required for the complete settling of sediment from the earlier event. A rough estimate of the maximum amount of time required for the settling of the finest particle component of sediment indicates that a complete graded bed would require about two days to form. (This estimation was calculated using the minimum settling rate of 25 minutes per meter that was derived from the clay component in the sediment accumulation research) (Fig. 17). Assuming that the basin was 40 m deep then the time for the clay to settle would be about 17 hours. The bed requires about 24 hours for consolidation following complete deposition (Fig. 15).

It is possible that the intermittent storms responsible for the *graded facies* depositional pattern were thunderstorms of variable strength that developed and initiated a pulse of precipitation and subsequent sedimentation into the GFS basin. Within the *graded facies*, the thickness and maximum grain size of the coarse component correlates with the total thickness of that graded-bed and indicates that the thickness of each graded-bed was a function of the energy (energy is the duration and amount of precipitation) of the corresponding depositional storm event. The total thickness of individual graded-beds ranges from 1mm to >2cm within close proximity, which indicates that conditions within the GFS were such that high-energy and low-energy depositional storm events were recorded within the sediment record. The *graded facies* is

composed of long sequences of individual graded beds, without intermediate deposition, which indicates that storms were the primary source of sediment into the GFS basin. If intermittent storms of variable strength were the primary source of sediment then it is likely those events were also the primary source of annual precipitation. Therefore, during deposition of >1m thick intervals, when the average thickness of a graded bed is about 1cm (Fig. 9a), either the environment received only a few storm events per year or the annual sedimentation rate was extraordinarily high. Considering the averaged thickness of the individual graded beds within the *graded facies* are ~ twice as thick as an entire couplet within the *laminated facies*, it would seem that each storm depositional event delivered a very high amount of sediment into the basin. There was likely a limit to the amount of annual sediment available within the watershed feeding the GFS. Although high sedimentation rates could be attributed to an unstable landscape, high paleorelief, limited vegetative cover, or some combination of factors, it is unlikely that the site received more than ~10 cm of fine-grained sediment (average maximum grain size is fine sand) per year. Therefore, an environment that receives precipitation from a limited number of storm events per year is likely a relatively dry environment.

In conclusion, the near perfectly normal size grading and the presence of rare interruptive beds within the *graded facies* appear to indicate that the "first flush" of deposition was not followed by additional minor depositional events or capable of exhausting the annual sediment load, and thus indicates that the individual graded beds within the GFS *graded facies* do not represent annual deposition. It is likely that an indefinite and variable number of individual graded beds represent an annual increment of sediment within the facies. The individual graded beds likely represent individual storm deposits that generated a "flush" of sediment into the GFS basin, and as the sediments settled they graded by particle size. The conditions within the site were such that graded beds of variable thicknesses were recorded within the stratigraphy, which appears to indicate that storms of variable energy were recorded within the sediment record. It is probable that the total thickness and amount of coarse particles within an individual graded bed indicates the duration and strength of storm events. In general, the individual graded beds are relatively thick, and although it is possible that multiple graded beds were deposited within a year, there are limits to the amount of sediment delivered annually. This suggests that the climate during the deposition of the *graded facies* was dry and the precipitation pattern was characterized by a few episodic storms per year. It is possible that the storms were generated seasonally with long hiatuses in deposition spanning most of the year, or that they were deposited episodically

throughout the year. The presence of interruptive beds indicates that at least some of the time depositional events were in close proximity.

II b. Transition from the *Laminated* to *Graded Facies*:

Up-section within the GFS sequence of sediments the *graded facies* is gradually succeeded by the *laminated facies*. The transition between the facies consists of four unique depositional patterns that include: 1) the thick, individual graded bed depositional pattern (thick dep. pat.) that characterizes the *graded facies* sediments (Fig. 9a), 2) the thin, individual graded bed and mixed, non-graded depositional pattern (thin/ mixed dep. pat.) (Fig. 9c), 3) the stochastic laminated depositional pattern (stochastic dep. pat.) (Fig. 9g), and 4) the laminated depositional pattern (laminated dep. pat.) that characterizes the *laminated facies* sediments (Fig. 8). The transition between the *graded facies* and *laminated facies* contains discrete depositional patterns, which indicates that they formed as a result of different depositional processes (Fig. 7b). The thick dep. pat. (Fig. 7a) has been interpreted to represent deposition from isolated storm events. The thin/ mixed dep. pat. (Fig. 7c) consists of thin (typically < 3 mm thick) graded beds that are intermittently interrupted with mixed non-graded sub-layers. The graded beds are thin likely indicating that they resulted from relatively lower-energy storm deposits. Throughout the GFS sediments the thickness of graded beds correlates with the amount and maximum size of the coarse component, which suggests the thickness of a bed is roughly correlated with the total amount of discharge from precipitation per storm event. Therefore, it is likely that the thin graded beds in the thin/mixed dep. pat. are the result of an average decrease in discharge per storm event. The presence of mixed silt and clay sub-layers with the thin/mixed dep. pat. suggests that the precipitation/ deposition pattern was more continuous than the thick dep. pat. The up-section trend within the thin/mixed dep. pat., whereby the thickness of graded beds decreases and the amount of mixed, non-graded sediment increases (Fig. 10), might indicate that precipitation/deposition pattern was becoming more continuous with less discharge per event.

The thin/mixed dep. pat. episodically interrupts the thick dep. pat. over several meters within the GFS stratigraphy, yet remains discrete (Figs. 6, 9b) throughout most of the transition this likely indicates that the differences between the depositional patterns were not related to mechanisms that required long amounts of time, or that cannot alternate back and forth in short amounts of time. Therefore, the thin/mixed depositional pattern was not likely related to gradual mechanisms of change such as: changes in the amount of available sediment, changes in watershed vegetative cover, changes in geomorphic relief, or to the filling and maturation of the

GFS basin itself. Additionally, the transition between the two facies is not consistent with rapid mechanisms of change such as: changing drainage patterns (avulsion), doline collapse, or other catastrophic events. Rather, the rhythmic alternation between depositional patterns appears to relate to two competing depositional processes. One of the competing processes correlates to the deposition of long sequences of thick graded beds, which dominate the stratigraphy from at least 485 m to ~ 497 m elevation, whereas the second process appears to first develop as the thin/ mixed dep. pat. and then to eventually evolve into the couplets that characterize the *laminated facies.*

The transition from the *graded facies* to the *laminated facies* is consistent with the development of a new precipitation pattern within the GFS watershed. The intermittent and apparently rhythmic alternation between the two depositional patterns, whereby the thin/mixed dep. pat. interrupts the thick dep. pat. in discrete intervals over several meters within the GFS stratigraphy, is consistent with two competing depositional patterns related to differing climatic forcing mechanisms. The thin/mixed dep. pat. appears to represent a new climatic mechanism of sedimentation characterized by more frequent precipitation events (thus increasing the amount of mixed sediment) with lower overall discharge (thus producing thinner graded beds). The thin/mixed dep. pat. does not originate as discrete couplets, which may indicate that either the new precipitation pattern was continuously developing up-section (thus the depositional pattern changed up-section accordingly), or that the new precipitation pattern was expanding into the GFS watershed and down-section sediments exhibit only partial control from the new forcing mechanism.

In conclusion, the transition from the *graded facies* to the *laminated facies* is recorded by sediments from ~ 497 m to 501 m elevation and is an important interval for understanding the up-section facies change within the GFS stratigraphy. There are two primary alternatives for the differences in depositional pattern between the facies. The first alternative is that changes to the GFS basin (such as doline collapse, filling up with sediment, changes in drainage (avulsion), changes in local or regional relief, eutrophication, or changes to the amount of vegetative cover) caused the development of the *laminated facies*, and the second alternative is that the precipitation pattern delivering sediment into the basin changed, thereby causing the development of the *laminated facies.* This facies transition is not consistent with fixed, unwavering, irreversible, gradual, or catastrophic mechanism of change such as; changes in drainage and subsequent sediment delivery into the basin, a filling basin, stream avulsion, changes in vegetative cover within the watershed, doline collapse, or geomorphic changes in basin stability.

The transition is consistent with the development and/or expansion of a new mechanism of sediment delivery relating to a changing precipitation pattern from climatic forcing. The development of the thin/mixed dep. pat. appears to represent the development of a more continuous precipitation pattern that episodically replaced the graded facies dep. pat. and eventually evolved into the couplets that characterize the overlying *laminated facies*. The thin/mixed dep. pat. is consistent with deposition from a series of relatively small rain events in close proximity to each other. During the intermediate periods between the depositional events the site likely continued to receive low-energy discharge that continuously deposited fine-grained, non-graded sediment into the basin. The thin/mixed dep. pat. did not originate as couplets, which may indicate that the new climate was either developing or expanding throughout the transitional sequence of GFS sediment.

II c. *Laminated Facies*

The consistent differences and the regular and continuous alternation between the (A) and (B) laminae indicate that the *laminated facies* had two distinct components within its depositional pattern. The (A) laminae consist of relatively poorly sorted, but well-mixed terrigenous clasts that include coarse sand-size clasts of organic debris and fine to medium sand-size quartz grains that are mixed in a silt and clay matrix. The (B) laminae are almost entirely composed of a silty-clay matrix and seldom have any sand-sized particles. The (A) laminae consistently contain larger grains, which indicate that a higher-energy depositional mechanism produced these laminae. This observation is also supported by the presence of pedorelict "rip-up" clasts that were derived from the local paleosols, which occur exclusively within the (A) laminae. These clasts are easily destroyed during transportation and therefore their presence indicates both a local origin and considerable amounts of energy to erode and entrain these clasts. The high-energy (A) laminae are typically thinner than the silty-clay (B) laminae, thus indicating that the high-energy depositional mechanism that produced the (A) laminae was of shorter duration relative to the lower-energy depositional mechanism that produced the (B) laminae.

Neither the (A) nor the (B) laminae are graded (Fig. 8), which suggests that they were not deposited in the same manner as the *graded facies*. When distinctly laminated sediments from the *laminated facies* were allowed to settle in a 25 cm water column the resulting beds were obviously graded (Fig. 7). Therefore, if the depositional mechanism producing the (A) and (B) laminae flushed large amounts of sediment into a water column that had >25 cm of calm water, then the sediments should have produced graded beds. It is difficult to envision a laterally

continuous sequence of laminated sediments being preserved in an environment inhabited by crocodilians, tapirs, and aquatic rhinoceroses, unless the water was relatively deep; therefore it is likely that the *laminated facies* sediments were not deposited in isolated events. Rather it is likely that the depositional mechanism that produced the *laminated facies* was more constant. As illustrated in Figure 8, the silty-clay (B) laminae consist of a thorough mixture of silt and clay clasts that are not sorted by size within any portion of the laminae. It is likely that the depositional pattern producing the (B) laminae was from a nearly constant sediment rain that consisted of exclusively fine particle sizes. The silty-clay matrix is also present within the organic-rich (A) laminae, but the (A) laminae also contain additional larger grains that, like the silty-clay matrix, are not sorted by size. This indicates that the silt and clay rain did not stop during the deposition of the (A) laminae, but rather that it continued and additional higher energy grains were added.

The alternating high-energy and low-energy depositional pattern that produced the *laminated facies* is consistent with a depositional model in which the (B) laminae represent relatively long intervals of deposition produced from a continuously flowing creek or river that gradually and continuously discharged silt and clay into the site, and during a relatively brief interval the creek discharge increased and the maximum particle size transported increased accordingly. During the periods of high discharge the creek cut into the local landscape, ripping up soil clasts and possibly organic debris, and entraining the clasts into the flowing water until they were eventually deposited into the GFS basin. Both the (A) and (B) laminae contain quartz derived from great distances to the east indicating that the sediment was ultimately derived from drainage from the east. The regular pattern of the alternating (A) and (B) laminae indicates that the high-energy period occurred in a consistent manner, and in nature consistent behavior is rare unless it relates to orbital forcing. The most plausible explanation for the *laminated facies* depositional pattern is that the (A) laminae represent drainage from a relatively short wet-season that added additional coarse sediment to the silty-clay background deposition. However, describing the (A) laminae as representing a seasonal depositional event implies that the couplets within the GFS laminated facies represent annual deposition (varves), and one must be careful not to assume, *a priori*, that a laminated sequence of sediment represents annual deposition.

There are many examples of ancient lacustrine sediments that are interpreted to be annual varves. Anderson and Dean (1988), and Anderson (1996) proposed that laminations are annual varves if one or more of the following criteria are met: 1) known seasonal associations of major and minor components; 2) an established chronology; 3) evidence for lateral continuity; and 4)

the cautious use of analogues. The preceding interpretation that the GFS *laminated facies* depositional pattern is seasonal with a high-energy wet season producing the coarse-grained, organic-rich (A) laminae and a relatively lower-energy season producing the silty-clay (B) laminae supports the interpretation that the GFS sediments are varves, but to use this interpretation of seasonal deposition as evidence would be a circular argument and is therefore not suitable. Due to the great age of the GFS ^{14}C dating is not possible, and there is currently no established high-resolution chronology for the site capable of supporting an argument for varves. The GFS sediments are laterally continuous everywhere they are exposed within the site, but the site is small (2.6 ha), and therefore lateral continuity at a scale similar to the correlation of glaciolacustrine varves over many kilometers is not possible. Therefore, although this evidence supports the interpretation that the GFS laminated facies is varved, it cannot be considered conclusive. The concept of an analogous environment to the GFS is complicated. Through my extensive literature review I could not find any well-documented modern environment similar to the GFS. This is interesting because sinkhole lakes are common and it would appear that modern sinkhole lakes could preserve valuable paleoclimatic records from variable terrestrial environments. Nonetheless, there does not appear to be a suitable modern environment to use as an analog for the GFS. However, some of the features of the GFS sediments can be analogous to both ancient and modern environments.

There are few natural phenomena that possess true periodicity, except for those related to astronomical cycles such as monthly tides or seasonal changes (Davis, 1986). The GFS contains statistically significant periodicity, which indicates that the deposition of the sediments occurred in a deterministic fashion. In a very small lake basin like the GFS it is difficult to envision any mechanism that could have produced the true periodicity, unless the couplets are varves. The math is complex but the SAS-ETS program makes it simple, and the method I followed was exactly the same as example one in the SAS users guide used to demonstrate Wolfer's 11-year sunspot periodicity. The only subjective part about the math or the method was the actual collection of the data. Typically, laminated sediments occur at a much smaller scale and/ or are not exposed in an adequate way to allow for manual field collection, therefore, the collection of a typical data set for spectral analysis is much more complex than within the GFS. However, random error in data collection would have detracted from the periodicity, and the data are very complex and would be nearly impossible to artificially create by inaccurate measurements. Therefore, it is not likely that the data are biased by errors in data collection. Thus the GFS periodicity should be reproducible by other researchers using a similar technique.

The 5-couplet periodicity derived from ~ 100 laminae recorded in sediment within the GFS *laminated facies* is likely analogous to the ~ 5-year cycle of Ripepe et al. (1991) and Crawley et al. (1986), which were derived from the distal "oil shales" of the Eocene Green River Formation. The 5-year periodicity was interpreted to represent the ENSO (El Niño, La Niña) phenomenon (Ripepe et. al., 1991), and 5-year periodicity within the GFS is therefore also interpreted to relate to ENSO disturbances. The sedimentological response to ENSO within the Green River Formation was attributed to either air masses coming in from the west (Fig. 21) or possibly related to monsoonal winds derived from the Gulf of Mexico. The presence of analogous periodicity between the Green River Formation and the GFS supports the hypothesis that the GFS *laminated facies* sediments are varves. Modern ENSO disturbances operate on a 3-7 year cycle and affect the amount of precipitation delivered to northeastern TN. Thus, precipitation cycles during the deposition of the GFS *laminated facies* may also have been controlled by ENSO disturbances, which may indicate that that the annual sedimentation rate within the *laminated facies* correlates with the amount of precipitation per year (which agrees with the previous interpretation that the thickness of individual graded beds within the *graded facies* correlate to the amount of precipitation per storm event).

Although the periodicity derived from the GFS appears analogous to the periodicity within the Green River Formation, neither the paleoenvironment nor the depositional patterns are analogous between the two sites. The Green River Formation was a very large Eocene lacustrine environment that contained a diverse assemblage of sediments, and the varved sediments are only present in specific distal portions. The Green River Formation varves alternate between illitic clay and kerogen in the lower part of the formation and between fine-grained precipitated carbonate and kerogen in the upper portions (Ripepe et al., 1991). The Green River Formation varves have been attributed to dominantly autochthonous deposition in which the thick, light-colored laminae were produced from carbonate precipitation during a higher-energy summer season that alternated with thinner laminae composed of kerogen from unknown origin; in contrast, the GFS *laminated facies* sediments contain organic-rich (A) laminae that alternate with silty-clay (B) laminae, and both laminae appear to be of allochthonous origin (Fig. 8). Therefore the continuously alternating depositional pattern of couplets between the two sites is similar; however, the origin of the sediment is vastly different. A better analogy of the depositional pattern within the GFS is the varved sediments from the northeastern Arabian Sea (Fig. 22). Rad and others (1999) described these sediments as dominantly terrigenous, and concluded that precipitation and river runoff control varve thickness. The couplets consist of light-colored, silty-

clay terrigenous laminae that alternate with a dark-colored, organic-rich, mixed biogenic and terrigenous laminae. The light-colored laminae are derived from eolian deposition during the winter (dry) Indian monsoon, and the dark-colored laminae are derived from the high-productivity summer (wet) monsoon. The dark laminae consist of a combination of terrigenous sediment and pelagic rain that forms as a result of the additional nutrient contributions during the Indian summer monsoon. Although the sediments differ greatly in terms of sediment sources and transport, in their observed periodicity, and in the sources of organic matter (Fig 22), they are the best analogy available for the depositional pattern observed within the GFS *laminated facies*.

In conclusion, the couplets within the GFS *laminated facies* appear to be representative of annual varves. The annual varve couplets continuously alternate between organic-rich, high-energy (A) laminae and silty-clay (B) laminae. The (A) laminae are interpreted to represent a distinct and abrupt wet-season that interrupted the deposition of the silty-clay matrix that composes the (B) laminae. The laminated facies depositional pattern appears continuous because the deposition of the silty-clay matrix was constant. Therefore, the gradual but continuous deposition of sediment into the basin likely indicates the site received a more continuous supply of water, which suggests that the *laminated facies* depositional pattern was related to a wetter climate than the *graded facies* depositional pattern. Thus, it appears as if the *graded facies* was deposited during a drier climate and the development of the thin/mixed depositional pattern represents the development of additional precipitation that increased and eventually developed into the wetter *laminated facies* depositional pattern.

Within the sequence of GFS laminated sediments a 5-year periodicity exists that can be attributed to an ENSO-like control on annual sediment thickness because the GFS lacustrine sediments appear to be dominantly allochthonous, and modern ENSO disturbances affect annual amounts of precipitation. Therefore, it appears that ENSO control on precipitation correlate with the annual amount of sediment delivered into the GFS basin. Thus, during wet years the thickness of annual varve couplets would increase relative to drier years. The ENSO variation may be attributable to winds from the west (Fig. 21) or possibly to upwelling in the Atlantic Ocean (discussed later). The best analog for the depositional pattern observed within the GFS *laminated facies* seems to be from the Arabian Sea anoxic sediments that are the result of seasonal variations from the Indian monsoon (Fig. 22). The presence of statistically significant ~5-year periodicity in the Eocene Green River Formation and the Early Pliocene GFS appears different than the modern 3-7 year cycle of ENSO (although the ~7 year spike within the GFS indicates a quasi-cycle that may relate to a less frequent and weaker 7 year ENSO cycle), and

although the depositional patterns of the Green River Formation and the Gray Fossil Site are different, both represent a seasonal climate, which may relate to the similar periodicity within each.

II d. Experimental modeling of GFS depositional patterns

A sediment accumulation experiment was conducted to model the differences in depositional pattern between the two lacustrine facies within the GFS. The experiment simulated the flush depositional pattern from the *graded facies* using sediment from the *laminated facies* couplets in order to understand the differences in depositional pattern as well as to determine the settling pattern of the sediments comprising the couplets.

In all four experiments the laminated facies sediments settled in a consistent manner and resulted in graded beds similar to the graded facies, which confirms that the two facies have different depositional patterns and that the individual graded beds within the GFS likely resulted from flushes of sediment deposited into the site. Two distinct suites of sediments, based on particle size and settling velocity, thus exist within the *laminated facies*. The coarse suite is comprised of large pieces of terrestrially derived organic matter, which had the highest settling velocity, and the sand-sized particles. The coarse suite is derived almost exclusively from the (A) laminae (Fig. 8), which indicates the (A) laminae likely represent deposition during a higher-energy season. A period of non-deposition (or very low deposition) separates the coarse suite from the fine suite (Fig. 16), and then the fine suite of sediment was deposited. The fine suite consisted of the silt and clay portion of the sediment that comprises the continuously deposited silty-clay matrix within the *laminated facies*. Within the experimental beds this portion of sediment is also graded which indicates that the silty-clay matrix was deposited in a gradual and continuous manner. After the developing experimental bed fully consolidated, the thickness of the coarse suite was ~ ½ the relative thickness of the average (A) laminae within the *laminated facies*, and this is because the (A) laminae consist of both the coarse suite and the silty-clay matrix, and therefore confirms that the deposition of the silty-clay matrix was continuous.

In conclusion, the sediment accumulation research consistently produced experimental beds with a similar depositional pattern to the *graded facies,* but generated from the *laminated facies* sediment. This indicates that the difference between the depositional patterns did not result from differences between sediment components. Thus, it is likely that the *laminated facies* depositional pattern was more continuous than the flush of sediment characterizing the *graded facies* depositional pattern. The coarse suite of sediment in the experimental beds was derived

almost exclusively from the (A) laminae, which indicate that it represents a higher-energy season that likely incised the local landscape, thereby liberating large pieces of terrestrial organic matter and soil aggregates for deposition into the basin.

II e. Sedimentation rates and rate of facies transition

Within the GFS vertical sequence of sediment the average bed thickness decreases up-section (Fig. 6). Within the transition from the *graded facies* to the overlying *laminated facies* this trend indicates that the average thickness of the individual graded beds decreases up-section, which indicates that the amount of thin/mixed depositional pattern sediment increased up-section. Within the *laminated facies* the average couplet thickness decreases up-section, and because the couplets are likely annual varves, this trend indicates that the annual amount of sediment delivered into the site decreased up-section. The average thickness of the individual graded beds within the *graded facies* is greater than the average thickness of the annual couplets within the *laminated facies,* which suggests that the sedimentation rate within the *graded facies* was extremely high. The up-section decrease in annual sedimentation may indicate that the amount of vegetation within the watershed increased (possibly related to the development of a wetter climate), that the sinkhole lake basin became more stable, that the amount of annual precipitation decreased through time (which is contrary to available data), or that the size of the basin was increasing. The normal trend in a filling basin is that the annual sedimentation rate increases as the accommodation space decreases up-section, but if the basin was shaped like an inverted cone then it is possible accommodation space increased up-section.

The majority of the transition from the *graded facies* to the overlying *laminated facies* occurs between an elevation of 498 m to 501.5m, and because evidence indicates the couplets within the *laminated facies* represent annual varves, it is possible to establish a sedimentation rate within this facies. The average thickness of the varve couplets (calculated from >10 adjacent couplets) decreases up-section within the vertical sequence (Fig. 6). The minimum average thickness of individual couplets was 0.41 cm per couplet and the maximum thickness of distinct couplets (at an elevation of about 502 m) was 0.71 cm. If each couplet represents one year and the sedimentation rate remained constant at the minimum average thickness of 0.41 cm then the climatic transition occurred in ~854 years. If the sedimentation rate remained constant at the maximum rate of 0.71 cm of sediment per year then the transition occurred in ~493 years. Therefore, the transition between facies probably occurred in less than 493 years, and this

estimate likely grossly overestimates the amount of time required for the *laminated facies* to develop.

II f. *Subaerial Facies*

Abruptly at an elevation of ~504.7 m the *laminated facies* ends and the *subaerial facies* begins (Fig. 5). The contact between the *subaerial facies* and the *laminated facies* is abrupt (occurring over a 3 cm interval) and likely indicates that the termination of the laminated sediments was not associated with shallow waters that are necessary for the development of subaerial exposure. It is unlikely that laminated sediments would be preserved in an environment with shallow water inhabited by abundant animals. Therefore, the deposition of lacustrine sediments may have continued for an undeterminable duration before the subaerial exposure of the lake bottom, and it is probable that pedogenic processes altered the upper portion of lacustrine sediment. It is possible that the original volume of lacustrine sediment was vastly decreased as pedogenesis oxidized large amounts of organic matter and removed most of the carbonate portion of the sediment.

The base of the *subaerial facies* is characterized by a paleoAlfisol, which typically requires ~ several thousand years to develop in forested environments (Birkeland, 1999). This indicates that for several thousand years after the GFS basin dried up the landscape was that of a forest. Above the Alfisol is another soil that appears to be associated with the Vertisol soil order, as described by Driese (pers. comm., 2002) and recognized by Smith (2003) which is present on the adjacent side of the GFS. Above the paleoVertisol there exists ~ 10 m of regolith that consists of colluvium and alluvial sediments, and the presence of this regolith indicates that the GFS basin remained a topographic low during this interval of deposition (Clark per. com., 2001; Smith, 2003).

In conclusion, the *subaerial facies* contains two distinct paleosols that overlie the *laminated facies* and likely indicate that the GFS eventually dried up for several thousand years, and then may have been returned to a lacustrine environment for an unknown duration of time. The transition from the laminated sediments to the paleoAlfisol is abrupt and indicates that part of the lacustrine record has been altered by oxidative pedogenic processes. The presence of a paleoAlfisol likely indicates a forest developed within the GFS basin for several thousand years, and a paleoVertisol with sporadic laminated beds, which appear to be similar to the laminated facies, exists above the paleoAlfisol and may indicate that the GFS basin eventually returned to a lacustrine environment that recorded a depositional pattern similar to that of the *laminated facies*.

III. APPROXIMATE %TOC AND STABLE CARBON ISOTOPES

III a. Approximate %TOC

The amount of organic matter abruptly increases within the vertical succession of GFS sediment between an elevation of 500.2 and 501.2 m as observed by a color change in field samples and an increase in the %TOC (Fig. 6). Using the sedimentation rate derived from the annual varve couplets at the base of the *laminated facies* to establish an estimate (likely an overestimate) of the amount of time required for this transition, it appears that the organic matter increased in ~ 150 years. Some of the additional organic matter consists of various sizes of pieces of allochthonous organic matter that appear to be derived from vascular plants. The pieces of organic matter are observed at the base of the latest (stratigraphically highest) thick individual graded beds and also within the stochastic sub-layers of sediment that eventually develop into the *laminated facies* couplets (Figs. 10b and 10c). The presence of allochthonous pieces of organic matter within the thick, graded beds indicates the depositional events producing the thick graded beds were capable of depositing organic matter into the GFS basin, which suggests the organic matter was not available in the watershed while the graded facies was deposited. The rapid increase in organic matter likely relates to changes within the GFS paleoenvironment that increased preservation or contributed additional organic matter, or alternatively, to a vegetative response to changing climate that increased the amount of available organic matter.

Paleoenvironmental changes that could have altered the organic matter record include eutrophication, the development of an anoxic or reduced oxygen bottom waters, or filling of the basin and loss of accommodation space. The GFS basin was small and it is unlikely that one part of the basin received drastically different sediment than others. Therefore, it is not likely that a filling basin was the primary mechanism for additional sediment. The preservation of precipitated pyrite and the original depositional fabric throughout the entire observed lacustrine sediment record indicates that the GFS maintained an anoxic or poorly oxygenated bottom, and although the hypolimnion depth may have increased and decreased, it is unlikely in such a small and shallow basin changes in lake chemistry would drastically effect the degradation of organic matter as it settled through the water column. The trophic state of the lake may have changed, thereby introducing additional sources of organic matter to the record. Petrographic analysis indicates that a large amount of the additional organic matter was allochthonous, but the small particle sizes cannot be successfully identified. Therefore, without C/N data demonstrating

otherwise, it is possible that part of the additional organic matter was derived from microbes or algae.

The increase in organic matter is concurrent with the development of the thin/mixed depositional pattern as the dominant depositional pattern into the lake, but this transition occurs several meters up-section of the trend whereby $\delta^{13}C$ values begin to become relatively negative and ~1m down-section from the development of the couplets that characterize the *laminated facies* depositional pattern (Fig. 6). The timing of this event within the stratigraphy may indicate that a wetter climate developed that promoted the development and/or preservation of organic matter within the GFS watershed.

In conclusion, the amount of organic matter within the GFS abruptly increases concurrently with the development of what appears to be a wetter climate. The increase likely occurs in ~150 years and appears to relate to the addition of large pieces of allochthonous organic matter to the GFS sediments. The presence of allochthonous organic matter within thick individual graded beds up-section likely indicates that the organic matter was not available, or that the paleoenvironment did not preserve organic matter during the deposition of the *graded facies*. Without C/N ratios it is not possible to determine if the source of the organic matter changed throughout the depositional history, or if considerable autochthonous contributions developed. The overall timing of the increase in organic matter and the petrographic identification of most of the additional organic matter as allochthonous may relate to the increased preservation and/or amount of vegetation within the GFS watershed caused by the development of a wetter climate.

III b. Stable carbon isotopes

Stable carbon isotope values derived from lacustrine sediment TOC can be a valuable proxy for vegetative changes in the watershed and for paleoenvironmental changes within the lake. Values of $\delta^{13}C$ derived from total organic matter can preserve paleoclimate and paleoenvironment records for millions of years (Meyers and Ishiwatari, 1993; Meyers, 1994). The three primary sources of organic matter incorporated into lacustrine sediments are the particle detritus of aquatic organisms (autochthonous), the residues from terrestrial plants surrounding the lake (allochthonous), and from the microbes that inhabit the water and sediments of lakes and the soil of the surrounding watershed (Meyers and Ishiwatari, 1993). C/N ratios derived from TOC enable the differentiation of autochthonous and allochthonous organic matter (Meyers, 1994), but

these data are currently unavailable for the GFS. Thus, both autochthonous and allochthonous sources of organic matter are considered.

Most photosynthetic plants including algae and vascular land plants, incorporate carbon into organic matter using the C_3, or Calvin Cycle pathway. This process discriminates against ^{13}C in favor of ^{12}C and produces a shift in $\delta^{13}C$ of about -20‰ from the inorganic carbon source. Other plants use the C_4, or Hatch-Slack photosynthetic pathway, which exerts additional energy in order to use CO_2 more efficiently and therefore incorporates more ^{13}C into organic matter than the C_3 pathway, producing a $\delta^{13}C$ shift of about -7‰ (Cerling et al., 1998). Modern, pre-anthropogenic atmospheric CO_2 has $\delta^{13}C$ values ~ -7‰, and C_3 and C_4 plants that produce organic matter from atmospheric CO_2 separate into distinctive suites. Land plants using the C_3 pathway have organic matter that averages approximately -27‰, whereas those using the C_4 pathway average about -14‰ (Meyers, 1997). Carbon isotope values for total organic matter in lacustrine environments reflect the sum of organic matter contribution to an environment and can therefore be used to differentiate between C_3, C_4, and mixed ecosystems.

Isotopic analysis of >20m of sediment from the GFS produced δ^{13} C values that ranged between -24‰ to -30‰. These values are consistent with dominantly C_3 plant contributions to the site (Fig. 6). Carbon isotope ratios of fossil tooth enamel from low latitudes (<37°N) indicate that C_4 plant ecosystems developed by 6 million years ago in Africa, South America, North America, and southern Asia (Cerling et al., 1997). North American records from high latitudes (>37°N) are restricted to the western half of the continent because of a lack of suitable Tertiary sediment records east of the Mississippi; available records show little evidence for C_4 plant biomass dominance at higher latitude (Cerling et al., 1997). At 36.5°N latitude, the GFS resides near this (arbitrary) boundary between high and low latitudes, but its location in east Tennessee places the GFS in a portion of North America where Tertiary carbon isotopic data were previously unavailable. If the Late Hemphillian age is accepted for the GFS, then the record of stable C isotope values represent the first data to examine the extent of the Early Pliocene spread of C_4 ecosystems into high latitudes east of the Mississippi river. The GFS carbon isotopic record indicates that C_3 plant-dominated ecosystems persisted into the Late Hemphillian. This interpretation is in agreement with previous studies that indicate that C_4 grasslands did not expand into northern high latitudes in North America, and extends the spatial significance of this assertion into the eastern half of the North American continent for the interval of time represented by the GFS sediments (latest Miocene-earliest Pliocene).

Although the $\delta^{13}C$ values within the GFS are consistent with a C_3 plant ecosystem throughout the entire 20 m record, there is considerable variation between the uppermost and lowermost 3 m of lacustrine sediment from which $\delta^{13}C$ values were derived. From 486 to 488 m elevation the *graded facie,s* averaged -24.8‰ where as values derived from 502.8 to 504.8 m elevation within the *laminated facie,s* averaged -29.1‰. This ~ 4‰ difference may indicate significant changes in the local vegetation, a change in the dominant source of organic matter (i.e., allochthonous or autochthonous), or to changes in conditions within the lake. The $\delta^{13}C$ values derived from the GFS lacustrine sediments cluster into three groups that include the *graded facies*, the transition between the graded and laminated facies, and the *laminated facies* (Fig. 18). Stable carbon isotope values from the entire *graded facies* are enriched (averaging -25.4‰ with samples as positive as -24.3‰) relative to the overlying *laminated facies* (averaging -29.3‰), and the transition between facies is characterized by what appears to be a generally linear trend in which values become more negative up-section (Fig. 6). The transition to more negative stable C isotope values up-section occurs concurrently with the emergence of thin-mixed depositional pattern, but >3m prior to the increase in %TOC (Fig. 6).

Lacustrine sediments throughout the GFS stratigraphy are dominantly composed of allochthonous clasts, and the organic matter within the *laminated facies* appears to be composed primarily of pieces of terrestrially derived vascular plants (allochthonous carbon). However, down-section within the *graded facies,* the amount and size of organic matter significantly decreases and organic matter identification becomes difficult, but the sediments are still dominantly composed of allochthonous material. Thus, the GFS organic matter may dominantly consist of allochthonous organic matter throughout the vertical succession of lacustrine sediment. The range of $\delta^{13}C$ values for C_3 plants can vary considerably from their average value of about -27‰; C_3 plant $\delta^{13}C$ values can become enriched to as high as -22‰ in water-stressed ecosystems and can become depleted to as low as -35‰ in dense forests with closed canopies (Cerling et al., 1997). Therefore, the transition from a relatively water-stressed ecosystem to wetter, forested ecosystem could explain the range of stable isotope values from between -24‰ to -30‰. Another possibility is that small amounts of C_4 plants existed within the ecosystem and contributed enriched organic matter to the record. Either C_4 contributions or relatively enriched C_3 organic matter would indicate a drier environment. Thus, if the organic matter from the entire GFS sediment is dominantly allochthonous, then the stable C record from the GFS is consistent with the interpretation, based on depositional pattern, that the ecosystem became wetter as the

laminated facies developed. However, the source of organic matter may have changed throughout the GFS depositional history from autochthonous to allochthonous contributions.

Autochthonous lacustrine organic matter can be derived from photosynthetic algae as well as from other microbes that inhabit the sediments within the lake. Photosynthetic algae are the dominant source of autochthonous organic matter to most lacustrine systems, and freshwater algae utilize dissolved CO_2, which is usually in isotopic equilibrium with atmospheric CO_2, and thus is typically indistinguishable from the range of C_3 of organic matter derived from the surrounding watershed (Meyers, 1994). However, there are situations for which dissolved CO_2 within a lacustrine environment is not in isotopic equilibrium with atmospheric CO_2. Depending upon the trophic state of a lacustrine environment autochthonous organic matter can shift $\delta^{13}C$ values more positive or more negative. As eutrophication increases, the organic matter may initially become more negative with a subsequent positive isotope excursion reflecting the changing relative contributions of ^{13}C-deleted microbial biomass relative ^{13}C-enriched photoautrophic biomass (Hollander and Smith, 2000). Thus, autochthonous lacustrine organic matter can be more positive or more negative than allochthonous organic matter. If the relative contributions of allochthonous and autochthonous organic matter or the trophic state of the lake changed throughout the depositional history of the site, it may explain the ~4‰ variation of $\delta^{13}C$ values observed within the vertical succession of sediment. C/N ratios or compound-specific $\delta^{13}C$ values derived exclusively from C_3 plants are necessary to determine the significance of the ~4‰ stable C isotope variation.

In conclusion, $\delta^{13}C$ values from total organic carbon derived from ~20m of GFS lacustrine sediment range between -24 and -30‰ and cluster into three distinct suites associated with different depositional patterns that define the *graded facies*, the *laminated facies*, and the transition between these facies. The $\delta^{13}C$ values are consistent with dominantly C_3 plant contributions and the organic matter within the *laminated facies* appears to be dominantly composed of allochthonous pieces of vascular plant debris. If the Late Hemphillian age is accepted for the GFS, then it appears that C_4 plants did not expand into northeastern TN during the Early Pliocene. The stable C isotope values become more negative up-section in the stratigraphy and do not correlate with the rapid increase in %TOC within the sediments, which indicates there is no correlation between that low %TOC and relatively positive values of $\delta^{13}C$ within the *graded facies*. The ~4‰ variation in $\delta^{13}C$ values derived from the bottom and top of the vertical succession of lacustrine sediment may be associated with the development of a wetter

ecosystem, as indicated by the facies transition, but additional C/N data are necessary to determine if the source of the organic matter changed throughout the depositional history.

IV. POSSIBLE MECHANISM FOR RAPID CLIMATE SHIFT

IV a. Climate shift

The results of petrographic, field stratigraphic, stable C isotope, and %TOC analyses of the uppermost 20m of GFS lacustrine sediment were evaluated previously in order to determine if the facies shift within the GFS stratigraphy is related to: 1) changes within the GFS basin as it matured and filled up, or 2) changes from the climatic forcing of sedimentation, or 3) some combination of factors. The transition from the *graded facies* to the overlying *laminated facies* is characterized by the episodic and somewhat rhythmic development of the discrete thin/mixed depositional pattern, which eventually evolves (up-section) into the couplets characterizing the *laminated facies* depositional pattern (Figs. 6, 10). This facies transition is not consistent with changes within a basin that is maturing and filling with sediment, but is consistent with the development and/or expansion of a new mechanism of sediment delivery relating to a more constant precipitation pattern from climatic forcing. The δ^{13} C values derived from the upper 20 m of GFS lacustrine sediment become ~4‰ more negative up-section within the stratigraphy (Fig. 6). This trend is consistent with a vegetative change within the GFS watershed from water-stressed values (at the base of the *graded facies*) to a forested environment with a slight canopy effect. However, the stable carbon isotope values may also have changed in response to changing relative contributions of allochthonous and autochthonous organic matter or to changes in the trophic state of the lake, and additional C/N data are necessary to determine if the source of the organic matter changed in the GFS basin. The amount of organic matter rapidly increases up-section and is concurrent with the facies shift (Fig. 6). Petrographic analysis revealed a large amount of the additional organic matter that consists of allochthonous pieces of vascular plants. The thick, graded beds that characterize the *graded facies* did not have visible pieces of organic matter derived from vascular plants until after the development of the thin/mixed depositional pattern, which suggests that the climate shift may have promoted an increase in the development and/or preservation of organic matter within the watershed. The GFS basin was small, relatively shallow, and appears to have maintained a poorly oxygenated bottom throughout its depositional history which likely indicates that neither the rate of organic matter degradation nor the distribution of sediment across the basin changed drastically through time. Although some of the data presented can be explained by a changing basin, the simplest explanation for the lacustrine

facies character, the facies transition, and the rapid increase in organic matter within the GFS is an abrupt climate shift that promoted the development of the *laminated facies* from the *graded facies*. The stable carbon isotope record may relate to a maturing basin becoming more eutrophic and/or to the response of vegetation to an increased amount of moisture.

IV b. Possible mechanism of climate shift

The results of petrographic, field stratigraphic, stable C isotope, and %TOC analyses of the uppermost 20m of GFS lacustrine sediment are all consistent with an abrupt climate shift whereby a relatively dry climate was episodically replaced by a wetter climate with a distinct high-energy season in <500 years. Both of the climates interpreted to exist within the GFS sediment record are different from the modern climate in northeastern TN, which is characterized by the constant delivery of >100 cm of mean annual precipitation. The driving mechanism for the apparent rapid climate shift may relate to the large-scale reorganization of the Atlantic Ocean during the Early Pliocene. If the Late Hemphillian age is accepted for the GFS then it is possible that the GFS lacustrine sediments were deposited contemporaneously during a brief episode of upwelling along the Atlantic Coast of North America, which occurred at the same latitude as the GFS (Fig. 23). The GFS contains quartz grains derived from ~80km to the northeast and ~20km to the southeast throughout its depositional history (Smith, 2003), which indicate the basin received drainage from the east, and this may have made the GFS sensitive to climate changes relating to the reorganization of the Atlantic Ocean.

The mechanism linking the possible concurrent Early Pliocene upwelling within the Atlantic to the climate in northeastern TN is complex, but may involve the difference between the modern Gulf-Stream current that transports warm equatorial waters along the Atlantic Coast of North America and the cold-waters associated with upwelling. In effect, the development of cold water associated with upwelling would create a high-pressure cell along the Atlantic Coast, whereas the modern coast maintains a low-pressure cell. The significantly similar North American geography suggests westerly winds, similar to modern westerlies, would have blown across the continent in the Early Pliocene. The presence of a high-pressure cell along the Atlantic coast may have affected the path of prevailing winds along the east coast of North America and may have changed the precipitation pattern in the region. In the mid-Miocene, eustatic sea-level changed in small cycles along the Atlantic coast (Riggs and Belknap, 1988), and if Early Pliocene sea-level operated in a similar pattern then it is possible that upwelling appeared episodically in response to eustatic increases. Thus, the potential for rapid and drastic climate change was

prevalent around the time the GFS was filling with sediment. In addition, *Gomphotherium* tusk growth and ungulate survivorship records indicate that seasonality of temperature and/or precipitation developed during the Late Miocene or Early Pliocene (Janis, 1989; Fox 2000), which may have further complicated the situation by creating a situation in which the continental temperature alternated between a seasonal low and high pressure cell relative to the cold Atlantic Ocean.

The depositional pattern within the *laminated facies* is characterized by a brief high-energy season that likely relates to an increase in discharge into the GFS basin from the watershed. The regularity of this high-energy season appears to match the depositional pattern produced by the modern Indian monsoon recorded in the Arabian Sea (Fig. 22, Table 6), and the GFS's *laminated facies* may have developed as a result of a small-scale monsoon wind system related to the brief episode of Early Pliocene upwelling in the Atlantic ocean, in combination with the development of seasonality of temperature. The 5-year periodicity recorded within the GFS appears to represent the ENSO phenomenon and is apparently analogous to the ~5-year periodicity recorded in the Eocene Green River Formation (Ripepe et. al., 1991). Interestingly, the strong 5-year periodicity varies from the modern 3-7 year ENSO periodicity which does not have a strong 5-year cycle. This may relate to a more direct expression of the ENSO mechanism within the GFS annual sedimentation rate resulting from ENSO control on the increase and decrease of upwelling strength, which would strengthen and weaken the pressure gradient between the Atlantic Ocean and North America.

6. CONCLUSIONS:

The Gray Fossil Site (GFS) appears to represent an ancient sinkhole lake fill that recorded a an interval of late Tertiary sedimentation. The overall fossil vertebrate fossil assemblage strongly suggests a Hemphillian age ($\geq$4.5 Ma) for the site (Parmalee et al., 2002), and the features on the aquatic rhinoceros *Teleoceras sp.* (Fig. 5) suggest a Late Hemphillian (4.5-5.5 Ma) age (Manning, 2003; Harrison and Manning, 1983). Analysis of ~20m of the uppermost GFS lacustrine sediment revealed three distinct facies that are differentiated by their depositional patterns, %TOC, and stable carbon isotope values (Fig 6). The *graded facies* (Fig. 9) occurs between 485m to ~497m elevation and is characterized by: (1) a nearly continuous succession of thick (~0.8cm) individual beds that normally size grade from fine sand to clay and are dominantly allochthonous sediment, (2) < 1%TOC, and (3) $\delta^{13}C$ values averaging -25.4‰; this facies is interpreted to represent episodic storm deposits in a relatively drier climate. The *laminated facies* (Fig. 12) occurs between ~501m to 504.8m elevation and is characterized by: (1) laterally continuous couplets averaging 0.4 to 0.6 cm thickness, with dominantly allochthonous non-graded sediment with a higher-energy, organic-rich (A) laminae added to the apparently continuous deposition of silty-clay matrix, (2) ~8 %TOC, and (3) $\delta^{13}C$ values averaging -29.3‰. The *laminated facies* is interpreted to represent a wetter climate with a nearly continuous discharge of water and sediment into the GFS basin. The depositional pattern is bi-seasonal with a distinct high-energy season characterized by coarser-grained sediment, large pieces of organic matter, and reworked soil aggregates entrained during local landscape incision. The base of the *subaerial facies* (Fig. 14) occurs at ~504.8m elevation and is characterized by a paleosol with features consistent with interpretation as a paleoAlfisol that developed on the upper-most lacustrine sediments, thereby oxidizing their organic matter and disrupting the original sediment fabric. The base of this facies is interpreted to represent the initial subaerial exposure and development of a forest within the GFS basin for several thousand years. The GFS $\delta^{13}C$ values ranged between -24 and -30‰, which is consistent with dominantly C_3 plant contributions to the organic matter record, and if the Late Hemphillian age is accepted, then these values indicate that C_4 grasslands did not expand into GFS watershed during the Early Pliocene.

The transition from the *graded facies* to the *laminated facies* is consistent with the development and/or expansion of a wetter climate characterized by a bi-seasonal precipitation pattern into the GFS watershed. This transition appears to have occurred in less than 500 years, and the increase in precipitation may have changed the amount and/or preservation of organic matter in the watershed, as well as shifted the stable carbon isotope values within the organic

matter to more negative values. However, additional C/N ratio data are necessary to determine if the relative contributions of allochthonous and autochthonous organic matter changed throughout the depositional history of the GFS. The mechanism responsible for the apparent climate shift may relate to possible contemporaneous upwelling in the Atlantic Ocean, which may have produced seasonally cold waters along the Atlantic coast of North America at roughly the same latitude as the GFS. The GFS *laminated facies* contains statistically significant 5-year periodicity, which appears to relate to the ENSO phenomenon.

REFERENCES CITED

REFERENCES CITED:

Anderson, R.Y. (1996) Seasonal sedimentation: a framework for reconstructing climatic and environmental change: in Kemp A.E.S., eds. Palaeoclimatology and palaeoceanography from laminated sediments: London, The Geological Society, p. 1-17.

Anderson, R.Y., Braddock L.K., Gardner, J.V. (1990) Expression of seasonal and ENSO forcing in climatic variability at lower than ENSO frequencies: evidence from Pleistocene marine varves off California: Palaeogeography, Palaeoclimatology, Palaeoecology, v. 78, p. 287-300.

Anderson, R.Y., Dean, W.E. (1988) Lacustrine varve formation though time: Palaeogeography, Palaeoclimatology, Palaeoecology, v. 62, p. 215-235.

Birkeland P.W. (1999) Soils and Geomorphology (3rd edition): New York, Oxford University Press, p. 430

Cande, S.C., Kent, D.V. (1995) Revised calibration of the geomagnetic polarity time scale for the Late Cretaceous and Cenozoic: Journal of Geophysical Research, v. 100, p. 6093-6095.

Cerling, T. E., Ehleringer, J. R., Harris, J. M. (1998) Carbon dioxide starvation, the development of C4 ecosystems, and mammalian evolution: Phil. Trans. R. Soc. Lond. Bull., v. 353, p. 159-171.

Cerling T.E., Harris, J.M., MacFadden, B.F., Leakey, M.G., Quade, J., Eisenmann, V., Ehleringer, J.R. (1997) Global vegetation change through the Miocene/ Pliocene boundary: Nature, v. 389, p. 153-158.

Coulombe, C.E., Dixon, J.B., and Wilding, L.P. (1996) Mineralogy and chemistry of Vertisols, in Ahmad, N., and Mermut, A. (eds.), Vertisols and technologies for their management: Developments in Soil Science 24: New York, Elsevier Pub. Co., p. 115-200.

Crawley, K.D., Duchon, C.E., Rhi, J. (1986) Climate record in varved sediments of the Eocene Green River Formation: Journal of Geophysical Research, v. 91, p. 8637-8647.

Davis, H.T. (1941) The analysis of economic time series: Principial Press, Bloomington, IN.

Davis, J.C. (1986) Statistics and data analysis in geology, John Wiley and Sons, New York, p. 258.

Durbin, J. (1967) Tests of Serial Independence Based on the Cumulated Periodogram, Bulletin of Int. Stat. Inst., v. 42, p. 1039-1049.

Farlow, J.O., Sunderman, J.A., Havens, J.J., Swinehart, A.L., Holman, J.A., Richards, R.L., Miller, N.G., Martin, R.A., Hunt, R.M., Storrs, G.W., Curry, B.B., Fluegeman, R.H., Dawson, M.R., Flint, M.E.T. (2001) The Pipe Creek Sinkhole biota, a diverse late Tertiary continental fossil assemblage from Grant County, Indiana: American Midland Naturalist, v. 145, p. 367-378.

Fox, D.L. (2000) Growth increments in *Gomphotherium* tusks and implications for late Miocene climate change in North America: Palaeogeography, Palaeoclimatology, Palaeoecology, v. 156, p. 327-348.

Fuller, W.A. (1976) Introduction to Statistical Time Series, John Wiley & Sons, Inc., New York.

Harrison, J.A., Manning, E.M. (1983) Extreme carpal variability in *Teleoceras* (Rhinocerotidae, Mammalia): Journal of Vertebrate Paleontology, v.3, p. 58-64.

Haug, G.H., Tiedemann, R. (1998) Effect of the formation of the Isthmus of Panama on Atlantic Ocean thermohaline circulation: Nature, v. 393, p. 673-676.

Hollander, D.J., Smith, M.A. (2001) Microbially mediated carbon cycling as a control on the $\delta^{13}C$ of sedimentary carbon in eutrophic Lake Mendota (USA): New models for interpreting isotopic excursions in the sedimentary record: Geochimica et Cosmochimica Acta, v. 65 p. 4321-4337.

Janis, C.M. (1989) A climatic explanation for patterns of evolutionary diversity in ungulate mammals: J. Palaeontol., v. 32, p. 463-481.

Kidinger, J. L., Davis, J.B., Flocks, J.G. (1996) Geologic controls on the formation of lakes in north-central Florida: in Pitman, J.K., Carroll, A.R. eds., Modern and Ancient Lake Systems, Utah Geological Association Guidebook 26, p. 9-30.

Manning (2003) on Kohl web page at http//members.aol.com/Graysite1/index.html.

Markwick, P.J. (1998) Fossil crocodilians as indicators of Late Cretaceous and Cenozoic climates: implication for using palaeontological data in reconstructing palaeoclimate: Palaeogeography, Palaeoclimatology, Palaeoecology, v. 137, p. 205-271.

Meyers P.A. (1997) Organic geochemical proxies of paleoceanographic, paleolimnologic, and paleoclimatic processes: Org. Geochem., v. 27, p. 213-215.

Meyers P.A. (1994) Preservation of elemental and isotopic source identification of sedimentary organic matter: Chemical Geology, v. 114, p. 289-302.

Meyers P.A., Ishiwatari, R. (1993) Lacustrine organic geochemistry- an overview of indicators of organic matter sources and diagenesis in lake sediments: Org. Geochem., v. 20, p. 867-900.

O'Brien, R.R. (1996) Shale lamination and sedimentary processes, in Kemp A.E.S., eds. Palaeoclimatology and palaeoceanography from laminated sediments: London, The Geological Society, p. vii- xii.

Owen, D. B. (1962) Handbook of statistical tables, Addison-Wesley publishing, Massachusetts, p. 424-426.

Parmalee, P.W., Klippel, W.E., Meylan, P.A., Holman, J.A. (2002) A Late Miocene-Early Pliocene population of *Trachemys* (Testundines: Emydidae) from east Tennessee: Annals of Carnegie Museum, v. 71, p. 233-239.

Pedersen, G.K. (1985) Thin, fine-grained storm layers in a muddy shelf sequence: an example from the Lower Jurassic in the Stenlille 1 well, Denmark: Journal of the Geological Society, London, v. 142, p. 357-374.

Picard, M.D., High, L.R. (1981) Physical Stratigrphy of Ancient Lacustine Deposits, in Ethridge, R.G., Flores, R.M., eds. Recent and ancient nonmarine depositional environments: Models for exploration, Society of Economic Paleontologists and Mineralolgists Spec. Pub. NO. 31, p. 233-260

Rad, V.U., Schaaf, M., Michels, K.H., Schulz, H., Berger, W.H., Siocko, R. (1999) A 5000-yr record of climate change in varved sediments from the oxygen minimum zone off Pakistan, Northeastern Arabian Sea: Quaternary Research, v. 51, p. 39-53.

Redwine, J.C. (1999) Not your typical karst: Characteristics of the Knox Group, southeastern US: Hydeogeology and Engineering Geology of sinkholes and Karst, Beck Pettit and Herring eds, 1999 Balkema, Rotterdam , ISBN 9058090469. p. 111-119.

Riggs, S.R., Belknap, D.F.(1988) Upper Cenozoic processes and environments of continental margin sedimentation: eastern United States; in Sheridan, R.E., and Grow, J.A., eds, The Geology of North America, Volume 1-2, The Atlantic Continental Margin, U.S., Geological Society of America, p. 131-176.

Ripepe, M., Roberts, L.T., Fischer, A.G. (1991) ENSO and sunspot cycles in varved Eocene oil shales from image analysis: Journal of Sedimentary Petrology, v. 61, p. 1155-1163.

Smith, S. (2003) M.S. thesis in progress: University of Tennessee.

Whisner, S. C., Hatcher, R.D. Jr., and Munsey, J. W. (2001) The possible link between east-west trending faults in the valley and ridge province of eastern Tennessee and the Gray fossil site: Geological Society of America Abstracts with Programs , v. 33, p. 59.

APPENDIX

Table 1: Stable carbon isotope compositions and %TOC from stratigraphic column (Fig. 6)

Station	$\delta^{13}C$ (V-PDB)	%TOC
TS #0	-29.7	8.12
505	-26.5	0.23
504.8	-28.3	2.15
504.5	-28.9	8.18
503.3	-29.3	5.83
502.8	-29.3	8.72
501.8	-29.6	9.18
500.1	-28.1	0.50
498.5	-27.5	0.42
497	-27.1	0.45
496	-25.7	0.40
495	-26.5	0.54
494	-25.0	0.60
493	-24.3	0.51
492	-27.0	0.38
491	-25.0	0.41
490	-26.3	0.33
489	-26.8	0.28
488	-24.6	0.38
487	-24.4	0.30
486	-25.4	0.36

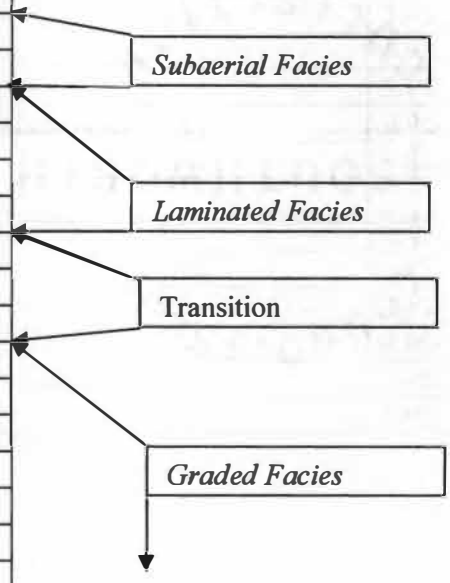

Graded Facies (486 to 497 m) mean = -25.8‰ and 0.4 %TOC
Laminated Facies (501.8 to 504.5 m + TS #0) mean = -29.4‰ and 8.0 %TOC
Transition (497 to 501.1) -27.6‰ and 0.46%TOC
Subaerial Facies (504.8 to 505) Only one data point and the transition were ran

Table 2: Stable carbon isotope compositions and %TOC from mechanically separated (A) and (B) laminae in sediment couplets from *laminated facies* (Fig. 18)

Laminated facies	$\delta^{13}C$	%TOC	m $\delta^{13}C$	m %TOC
(A) #1	-29.0	15.0		
(A) #2	-29.1	15.6		
(A) #3	-29.4	17.5		
(A) #4	-29.2	17.2		
(A) #5	-29.0	18.7	(A) mean=	(A) mean=
(A) #6	-28.7	14.2	-29.0	15.1
(B) #1	-29.6	6.1		
(B) #2	-29.1	10.5		
(B) #3	-29.1	4.2		
(B) #4	-29.8	6.3		
(B) #5	-29.4	5.9	(B) mean =	(B) mean =
(B) #6	-29.8	6.1	-29.5	6.5

Table 3: Periodicity raw data (Figs. 11, 19)

Rank	Cumulative distance (cm)	(A) laminae thickness (cm)	Thickness between adjacent needles(cm)
1	0.0	0.40	0.40
2	0.40	0.10	0.50
3	0.90	0.10	0.45
4	1.35	0.40	0.75
5	2.10	0.10	0.50
6	2.60	0.20	0.50
7	3.10	0.50	1.30
8	4.40	0.70	1.30
9	5.70	0.50	0.70
10	6.40	0.40	1.00
11	7.40	0.90	0.75
12	8.15	0.80	1.60
13	9.75	0.80	1.00
14	10.75	0.40	0.65
15	11.40	0.40	0.70
16	12.10	0.60	1.00
17	13.10	0.65	0.90
18	14.00	0.60	0.80
19	14.80	0.40	0.40
20	15.20	0.20	0.40
21	15.60	0.20	0.30
22	15.90	0.10	0.50
23	16.40	0.10	0.60
24	17.00	0.50	0.40
25	17.40	0.20	0.25
26	17.65	0.10	0.60
27	18.25	0.50	0.55
28	18.80	0.15	0.40
29	19.20	0.15	0.30
30	19.50	0.20	0.75
32	20.25	0.55	0.35
33	20.60	0.20	0.20
34	20.80	0.10	0.30
35	21.10	0.10	0.50
36	21.60	0.70	1.20
37	22.80	0.10	0.80
38	23.60	0.40	0.40
39	24.00	0.10	0.50
40	24.50	0.10	0.40

Table 3. Continued.

Rank	Cumulative distance (cm)	(A) laminae thickness (cm)	Thickness between adjacent needles(cm)
41	24.90	0.10	0.20
42	25.10	0.10	0.30
43	25.40	0.10	0.45
44	25.85	0.10	0.30
45	26.15	0.15	0.35
46	26.50	0.10	0.50
47	27.00	0.30	0.50
48	27.50	0.25	0.70
49	28.20	0.50	0.75
50	28.95	0.50	0.45
51	29.40	0.10	0.50
52	29.90	0.10	0.50
53	30.40	0.50	0.60
54	31.00	0.50	0.60
55	31.60	0.10	0.40
56	32.00	0.60	0.75
57	32.75	0.40	0.35
58	33.10	0.10	0.40
59	33.50	0.30	0.50
60	34.00	0.10	0.80
61	34.80	0.30	0.70
62	35.50	1.30	1.75
63	37.25	0.50	1.25
64	38.50	0.90	0.55
65	39.05	0.10	0.45
66	39.50	0.25	0.50
67	40.00	0.15	0.90
68	40.90	0.60	0.70
69	41.60	0.40	0.3
70	41.90	0.10	0.4
71	42.30	0.25	0.35
72	42.65	0.20	0.65
73	43.30	0.25	0.40
74	43.70	0.10	0.75
75	44.45	0.90	0.75
76	45.20	0.15	0.55
77	45.75	0.10	0.40
78	46.15	0.20	0.40
79	46.55	0.10	0.35
80	46.90	0.10	0.30
81	47.20	0.15	0.45

Table 3. Continued.

Rank	Cumulative distance (cm)	(A) laminae thickness (cm)	Thickness between adjacent needles(cm)
82	47.65	0.10	0.45
83	48.10	0.20	1.00
84	49.10	1.30	0.90
85	50.00	0.10	0.50
86	50.50	0.10	0.75
87	51.25	0.70	1.25
88	52.50	1.20	1.00
89	53.50	0.10	0.60
90	54.10	0.40	0.90
91	55.00	0.40	1.10
92	56.10	0.70	0.60
93	56.70	0.40	0.60
94	57.30	0.60	0.55
95	57.85	0.40	0.55
96	58.40	0.30	0.70
97	59.10	0.50	0.50

Table 4: Couplet thickness of *laminated facies*

Couplet #	Couplet thickness(cm)
1	2.2
2	4.75
3	4.05
4	2.10
5	3.25
6	6.10
7	4.15
8	4.30
9	7.65
10	5.15
11	4.90
12	2.40
13	3.40
14	4.35
15	4.00
16	1.80
17	3.15
18	2.55

Mean	Std. Dev
3.902778	1.504745

Table 5: Thickness of (A) and (B) laminae

Thickness (A) (cm)	Thickness (B)
0.55	1.40
0.50	4.30
0.80	3.50
0.80	1.65
0.45	2.95
0.30	3.70
2.85	3.65
0.65	3.65
0.75	3.60
4.90	5.25
0.70	2.40
0.60	2.55
0.40	3.40
0.75	3.55
1.05	1.10
0.40	1.25
1.50	2.30
0.15	

Mean	Std. Dev.	OL/10cm
1.005556	1.14145	25*

Mean	Std. Dev.
2.952941	1.151964

* In the 7.6 cm represented by Thin-section #0 there are 19 OL, therefore in 10cm there would be 25 OL

Table 6: Raw data for sediment accumulation: tests 1-4 in cm (T-1=test #1; T-1C=test#1 corrected)

Seconds	Minutes	T-1	T-2	T-2C	T-3	T-3C	T-4	T-4C
10		1.0	11.0	0.0	19.5	0	26.0	0
20					21.0	1.5		
30		2.5					27.0	1.0
40								
50			13.0	2.0	22.0	2.5		
60	1	3.0			22.4	2.9	28.5	2.5
120	2	3.2	14.0	3.0	22.6	3.1	28.3	2.3
180	3	3.2	14.0	3.0	22.6	3.1	28.0	2.0
240	4		13.5	2.5	22.3	2.8	28.1	2.1
300	5	3.0	13.0	2.0	22.0	2.5	28.0	2.0
360	6		14.0	3.0	22.3	2.8	28.0	2.0
420	7	3.4	14.2	3.2	22.0	2.5	28.2	2.2
472	8	4.0	14.5	3.5	22.5	3.0	28.0	2.0
540	9	5.0			23.0	3.5	28.5	2.5
600	10	6.0	15.2	4.2	23.6	4.1	29.0	3.0
660	11	6.9	15.6	4.6	24.0	4.5		
720	12	8.3	16.3	5.3	24.3	4.8	29.9	3.9
780	13	9.5	17.2	6.2	24.8	5.3		
840	14	11.6	17.3	6.3	25.2	5.7		
900	15	11.8	18.2	7.2	26.0	6.5	30.9	4.9
960	16	13.0	19.5	8.5	26.3	6.8		
1020	17	14.0	19.9	8.9	26.9	7.4		
1080	18	15.2	20.6	9.6	27.3	7.8		
1140	19	15.5	21.7	10.7	28.1	8.6		
1200	20	17.5	22.3	11.3	28.5	9.0	33.5	7.5
1260	21	18.8	23.0	12.0	29.2	9.7		
1320	22	20.0	23.8	12.8	30.0	10.5		
1380	23	21.1	24.5	13.5	30.5	11.0		
1440	24	21.9	25.3	14.3	31.0	11.5		
1500	25	23.2	26.3	15.3	31.8	12.3	36.4	10.4
1560	26	24.1	27.0	16.0	32.2	12.7		
1620	27	25.0	28.0	17.0				
1680	28	25.1	29.0	18.0	33.6	14.1		
1740	29	25.8	29.8	18.8				
1800	30	25.4	30.5	19.5	35.0	15.5	39.8	13.8
1860	31							
1920	32							
1980	33							
2040	34							

Table 6 Continued

Seconds	Minutes	T-1	T-2	T-2C	T-3	T-3C	T-4	T-4C
2100	35		35.0	24.0	38.1	18.6	42.9	16.9
2160	36							
2220	37							
2280	38							
2340	39							
2400	40						46.0	20.0
2460	41							
2520	42							
2580	43							
2640	44							
2700	45	27.5	42.8	31.8	44.0	24.5	49.9	23.9
2760	46							
2820	47							
2880	48							
2940	49							
3000	50				47.8	28.3	53.0	27.0
3060	51							
3120	52		46.5	35.5				
3180	53							
3240	54							
3300	55						57.0	31.0
3360	56							
3420	57							
3480	58							
3540	59							
3600	60	25.4	46.5	35.5	52.5	33.0	60.0	34.0
7200	120	21.5	36.0	25.0	47.0	27.5	57.5	31.5
21600	360						51.5	25.5
72000	1200	15.5	22.3	11.3	31.6	12.1	42.5	16.5

Table 7: Settling time for GFS clay component.

Minutes after deposition	Settling time for 3cm	Conversion to meters
37.0	19.7sec	10.8min
37.5	22.1sec	12.3min
38.0	22.7sec	12.6min
42.0	29.3sec	16.3min
43.0	20.3sec	11.3min
44.0	27.6sec	15.3min
51.0	32.3sec	17.9min
52.0	30.3sec	16.8min
53.0	45.0sec	25.0min

Table 8: Comparison of GFS, Green River Formation, and modern Arabian Sea varved depositional patterns (Fig. 22)

Characteristic	Gray Fossil Site	Green River Formation	Modern Arabian Sea
Basin	Small sinkhole lake	Large lake	Arabian Sea (700 m depth)
Dark laminae description	Organic rich, poorly sorted, terrigenous sand to clay	Kerogen	Organic rich, poorly sorted fossil rich, silt and clay
Light laminae description	Well sorted, terrigenous silt and clay.	Lower illitic clay; Upper precipitated carbonate	Well sorted terrigenous silt and clay
Couplet size	About 4 to 7 mm	Microscopic	About 0.8 to 1.5 mm
Source	Stratified anoxic	Stratified anoxic	Oxygen minimum zone
Origin dark laminae	Terrestrial	Phytoplankton (Nectoplanktonic)	Mixed biogenetic, terrestrial
Climate dark laminae	High-energy season	Dry season, low energy season (?)	Wet summer monsoon
Origin light laminae	Terrestrial	Biogenic carbonate- upper Spring flood- lower	Terrestrial eolian
Climate light laminae	Low-energy season	Wet, high energy monsoon or westerly winds (?)	Windy winter monsoon
Periodicity	5- ENSO	4.8-5.6 (c e. 5)- ENSO 10.4- 14.7- Sunspot	250- (?) 125-(?) 95- Gleissberg solar 56- (?) Only very weak ENSO
Thickness light/ Thickness dark	3.0	NA	0.7

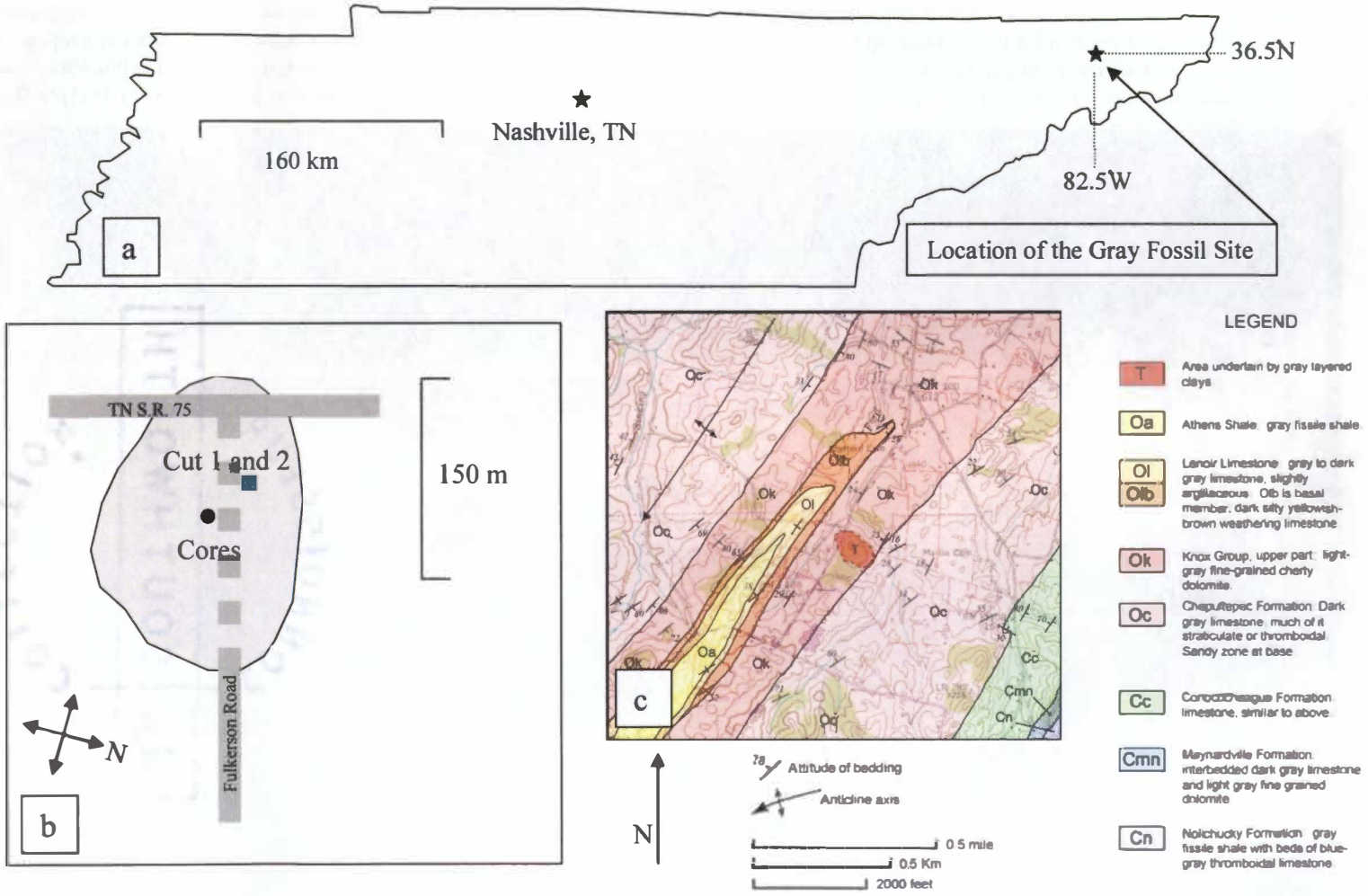

Fig. 1. Maps of the Gray Fossil Site (GFS), Tennessee: Fig 1(a). Location of the GFS. Fig 1(b). Schematic drawing of the GFS including the location of the Cores and Cuts 1 and 2. Fig 1(c). The GFS area (Modified from Kohl 2003). The GFS resides on a fold-limb in the Cambro-Ordovician Knox Group dolostone (Ok).

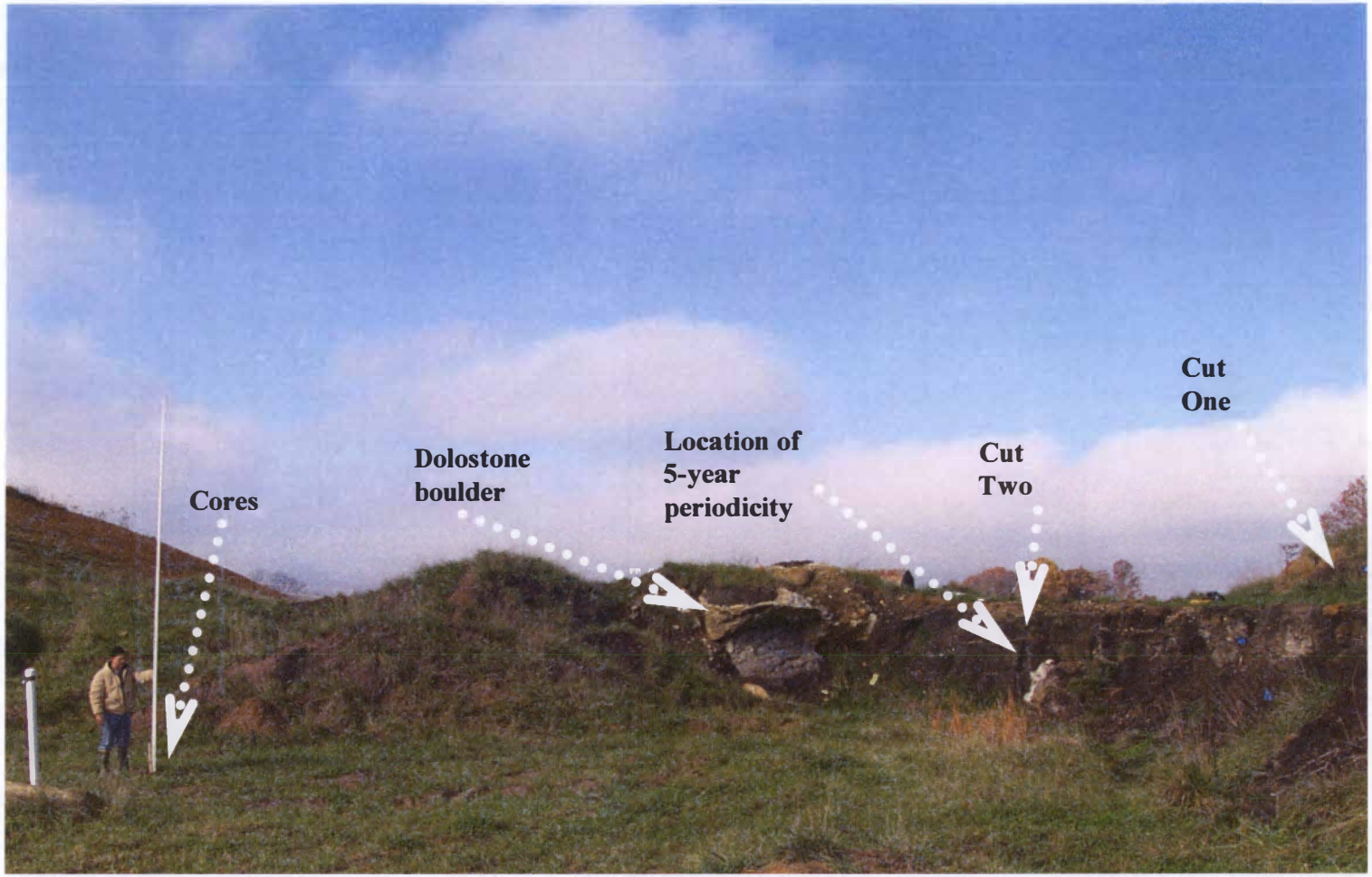

Fig. 2. Gray Fossil Site (GFS) research sampling locations: Photograph of the north-west edge of the GFS exposure, showing sampling sites. The measuring rod in the bottom left corner is 5 m in length. The white arrows indicate the sampling locations of Cut-One, Cut-Two, and Cores, as well as the location sample yielding sediment complete with 5-year periodicity was found. Notice the large dolostone boulder in the center of the photograph. To the right of the boulder is a large exposure of the dark-colored, unlithified *laminated facies* sediments.

Fig. 3. Gray Fossil Site unlithified lacustrine sediment: Photograph of the northwestern edge of the GFS exposure. The measuring rod is 5 m in length and is positioned vertically parallel to Cut-Two. Notice the laterally continuous chert/ dolostone layers; these layers were not visible during early excavation. Notice the several large boulders, the largest boulder is the same from Fig. 1.

Fig. 4. Field photographs of Cut-One and Cut-Two: Fig. 5(a) Photograph of Cut one; the red-flag is positioned at an elevation of 500 m. Inset- Notice the abrupt transition from the dark-colored *laminated facies* to the oxidized paleosol that marks the *subaerial facies*. Fig. 5(b) is a close up of Cut-Two; notice that the laminated sediments are laterally continuous. Data for periodicity were taken below the upper chert/ dolostone layer (below hand).

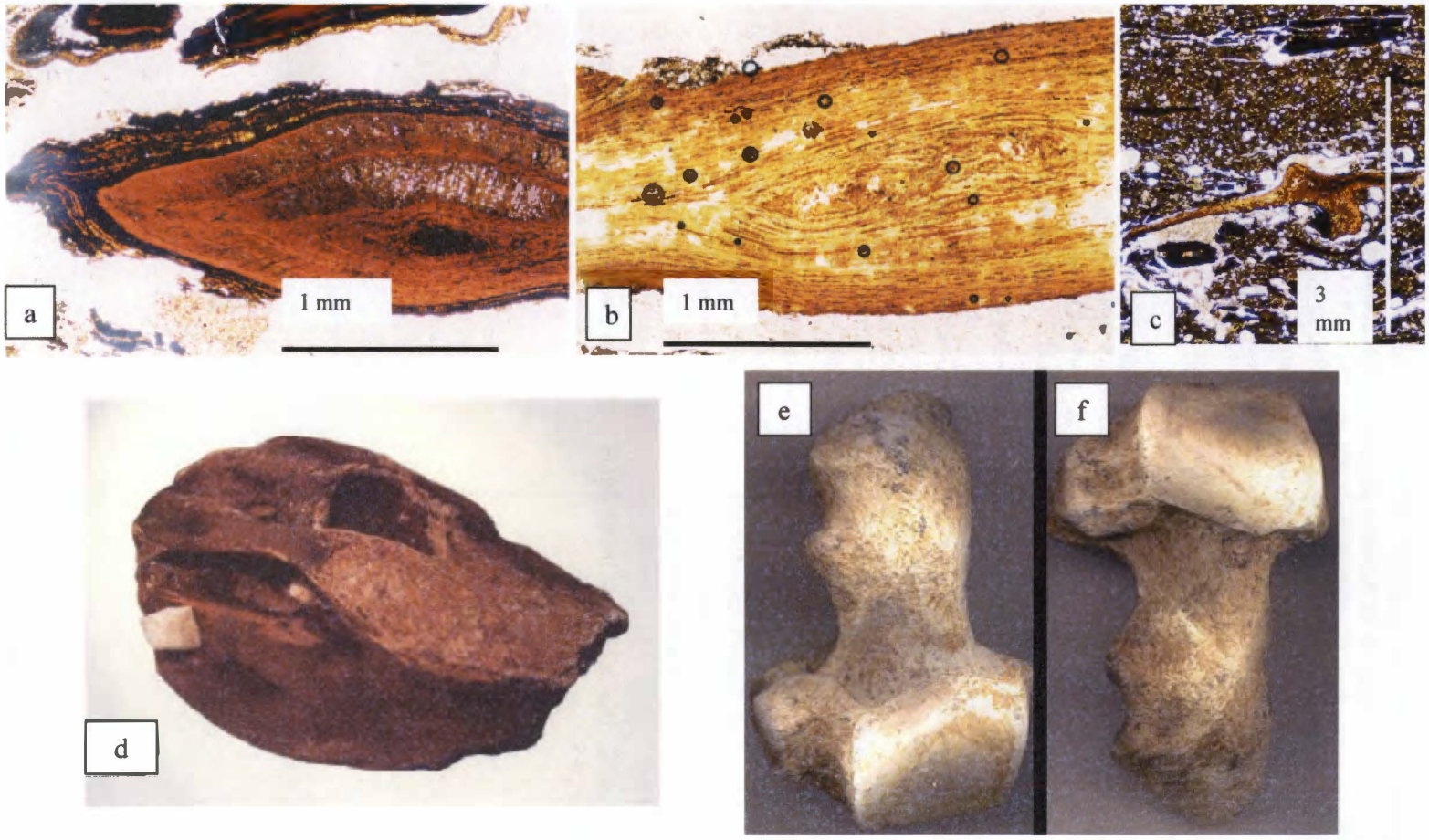

Fig. 5. Gray Fossil Site (GFS) fossils and preservation: Fig. 5(a) and 5(b) are photographs of pieces of GFS plant organic matter in thin-section at 5x mag. Notice the vascular structure and superb preservation. Fig. 5(c) is a photograph of a vertebra from an unidentified fossil in thin-section at 2x mag. Fig. 5(d) is a skull from an adult crocodilian; the presence of crocodilians indicates that the coldest month mean temperature for the GFS was >5.5°C (Markwick, 1998). Fig. 5(e) and 5(f) are photographs of the proximal view of the right and left unicoforms from *Teleoceras*. The presence of medial projections on both unicoforms indicates a Late Hemphillian age for the GFS (Manning, 2003). Photographs 5(d), 5(e), and 5(f) are courtesy of Martin Kohl and are available on the web at **http//members.aol.com/Graysite1/index.html.**

Fig. 6. Stratigraphy of the Gray Fossil Site (GFS): (Left to Right) Stratigraphic column (far left); Three distinct facies occur in the the upper 20m of lacustrine sediment in the GFS. The *graded facies* occurs between an elevation of about 486 m to 497 m. The *laminated facies* occurs between an elevation of about 501 m to about 504.8 m. The *subaerial facies* initiates at an elevation of about 504.8 m and persists until the top of the deposit. The transition from the *graded facies* to the *laminated facies* occurs between an elevation of about 497 m to 501 m. This transition is marked by the development of the thin/mixed depositional pattern. This depositional pattern eventually evolves into the *laminated facies*. The brief interval marked "no data" represents the lost portion of core.

$\delta^{13}C$ (V-PDB) values of organic matter (Table one). Isotopic compositions range from –24.3 to –29.6‰, and generally tend to become more negative up-section. Vertical stippled line at –27‰ indicates the average value of C_3 plants (Cerling et al., 1997). The thick stippled line indicates the a lack of data due to a covered interval between field cut-two and the cores.

Approximate weight %TOC values analyzed from the same samples analyzed for $\delta^{13}C$ (organic matter). The *graded facies* contains on average less than 1 %TOC whereas the *laminated facies* averages 8%TOC. The thick stippled line represents a covered interval. Because the cores were collected from about 25 m away from Cut-two, it is unclear what role spatial and temporal variance each played in the increase of %TOC. Samples collected in a vertical sequence beneath cut-two show a distinct color-change at an elevation from 500 to 501 m, which appears to indicate that the increase in %TOC is the result of up-section temporal changes.

Bed Thickness; The average thickness of individual graded beds within the *graded facies*. Thickness decreases up-section, the result of the initiation and ever-increasing abundance of the thin/ mixed depositional patterns. Within the *laminated facies* the average thickness of individual couplets decreases up-section within the stratigraphy. This trend likely results to a decreased amount of annual sediment from increasing vegetative-cover or to decreasing relief in the local environment.

Oriented Thin-Sections; This table shows the elevation of the 14 oriented thin-sections that were collected from the GFS.

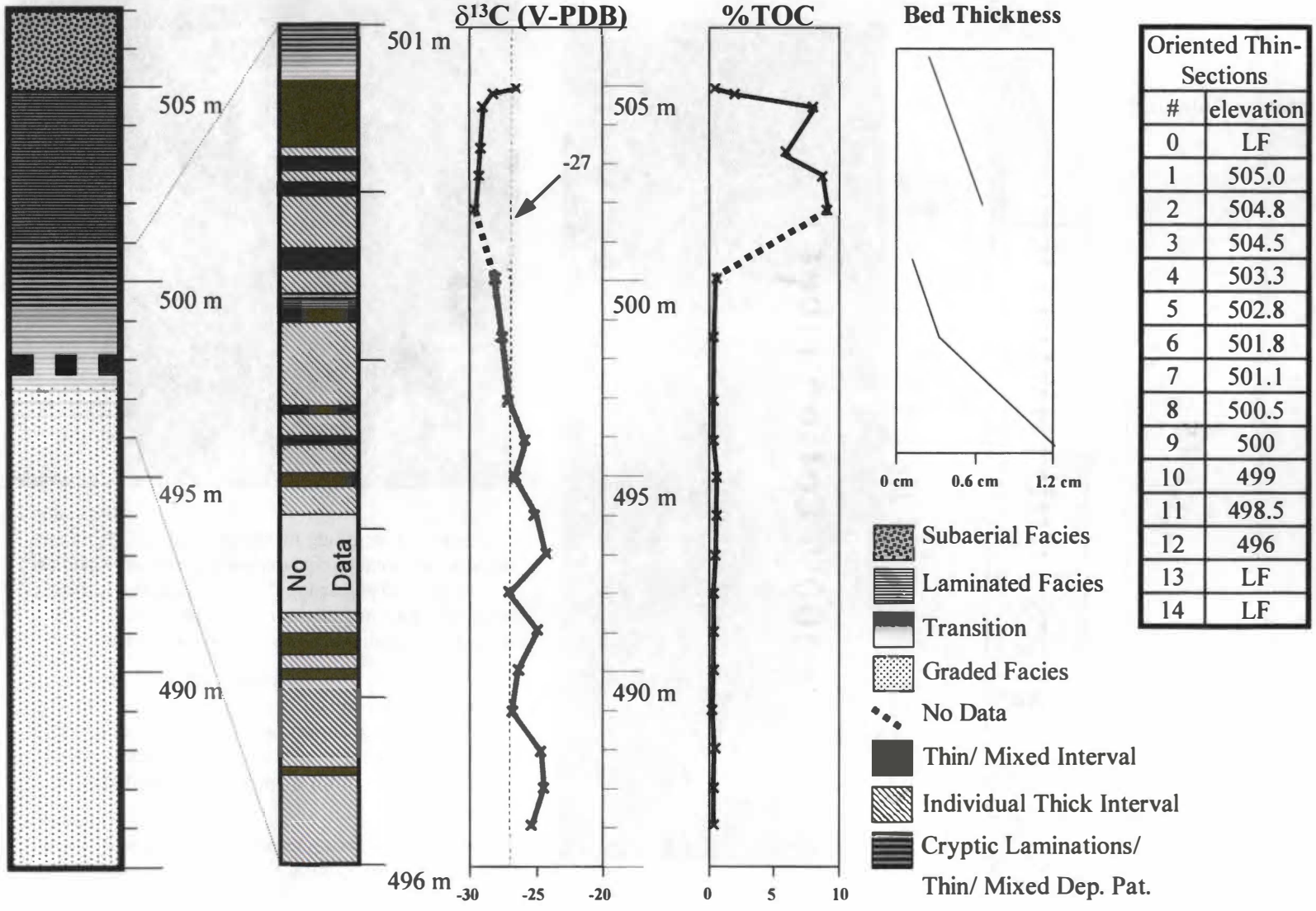

Oriented Thin-Sections	
#	elevation
0	LF
1	505.0
2	504.8
3	504.5
4	503.3
5	502.8
6	501.8
7	501.1
8	500.5
9	500
10	499
11	498.5
12	496
13	LF
14	LF

Fig. 7. Settling column: The picture (middle) is of the settling column used to conduct the sediment accumulation research.

The diagram (right) shows the 6.6 cm diameter of the column. Laminated sediments from the GFS (Fig.8) were settled through 1 m of water. During the process the thickness of beds accumulating on the bottom of the column were measured and recorded.

The picture (left) shows the result of similar study where sediments were settled through a 0.25 m water column at variable increments of time. Notice that the beds are normally size-graded, and how the thickness of beds was altered by varing the amount of time allowed between deposition.

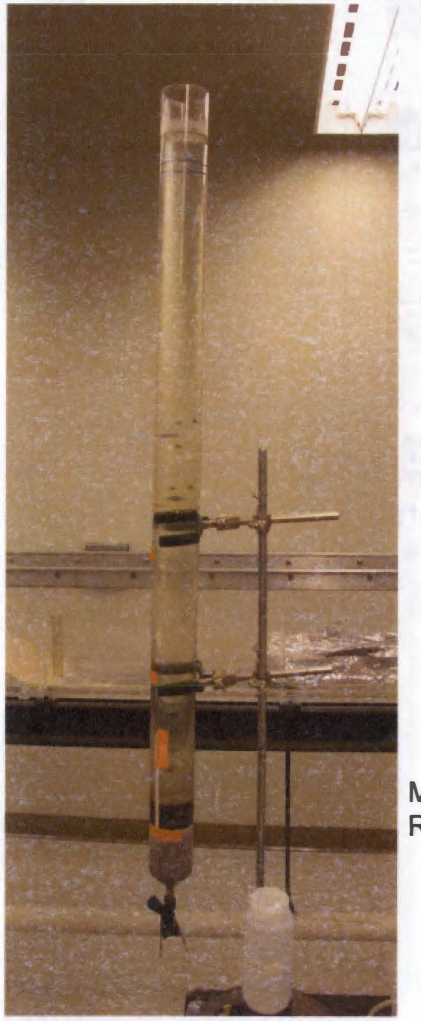

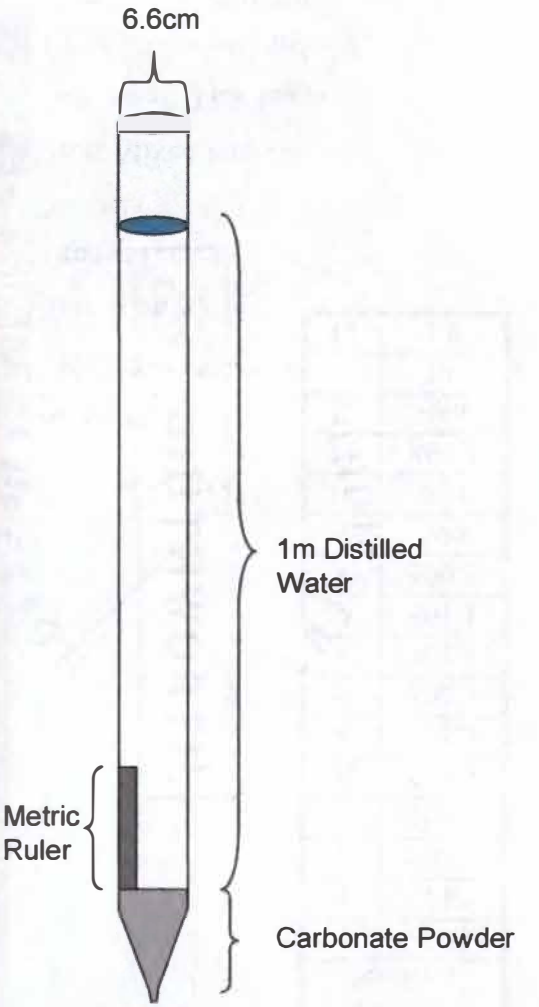

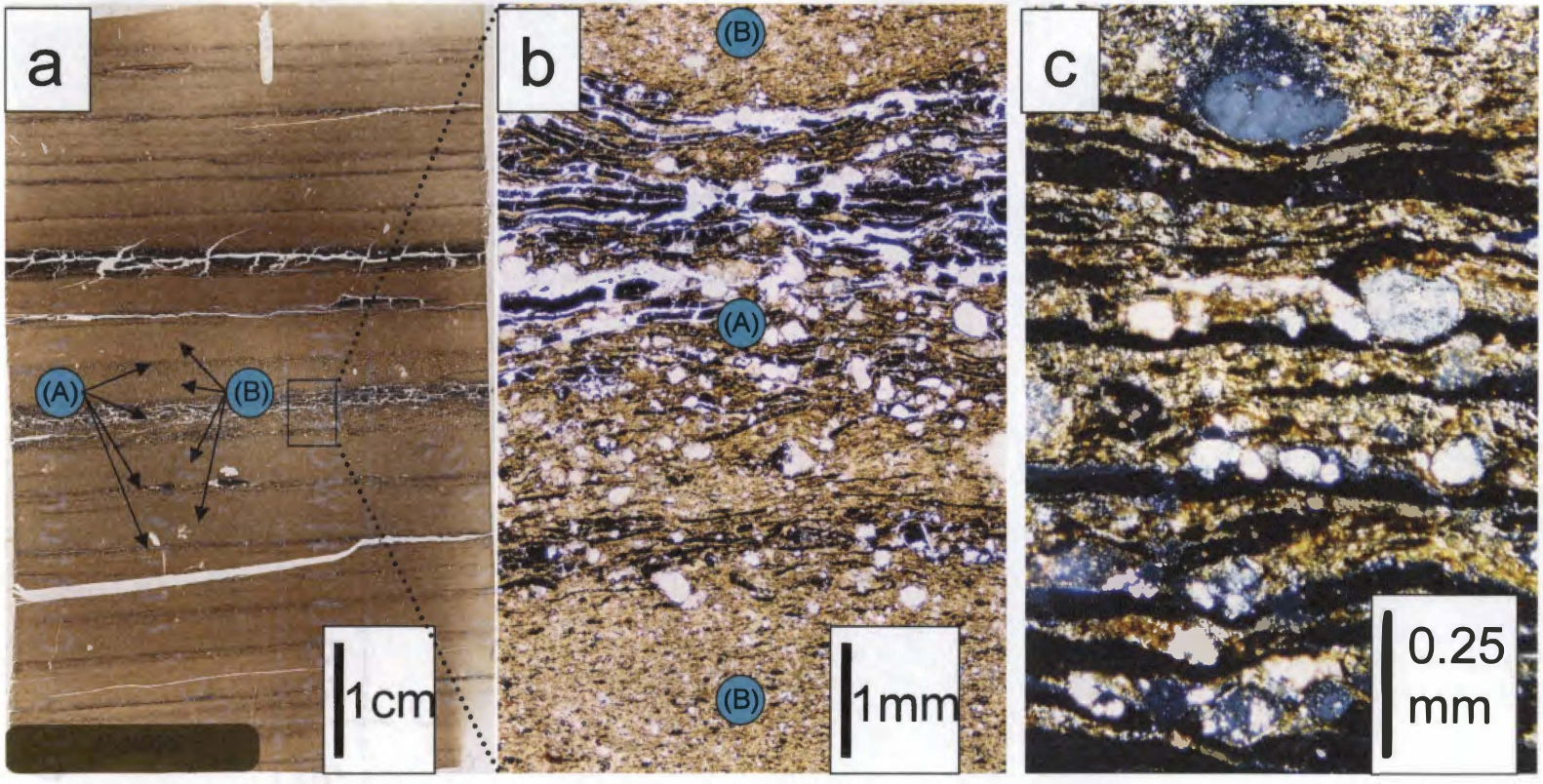

Fig. 8. Petrography of distinctly laminated sediments: 8(a). Thin-section from the GFS *laminated facies,* which contains laminations that are composed of alternating high-energy (A) laminae with silty-clay (B) laminae, interpreted to be annual varves.

8(b). The (A) laminae consist of coarser-grained clasts and more organic matter compared to the (B) laminae.

8(c). The (A) laminae are not graded and are poorly sorted with clay, silt, and sand sized clasts. Also note there are silty-clay sub-layers mixed within the (A) lamina, as are apparent in both 8b and 8c.

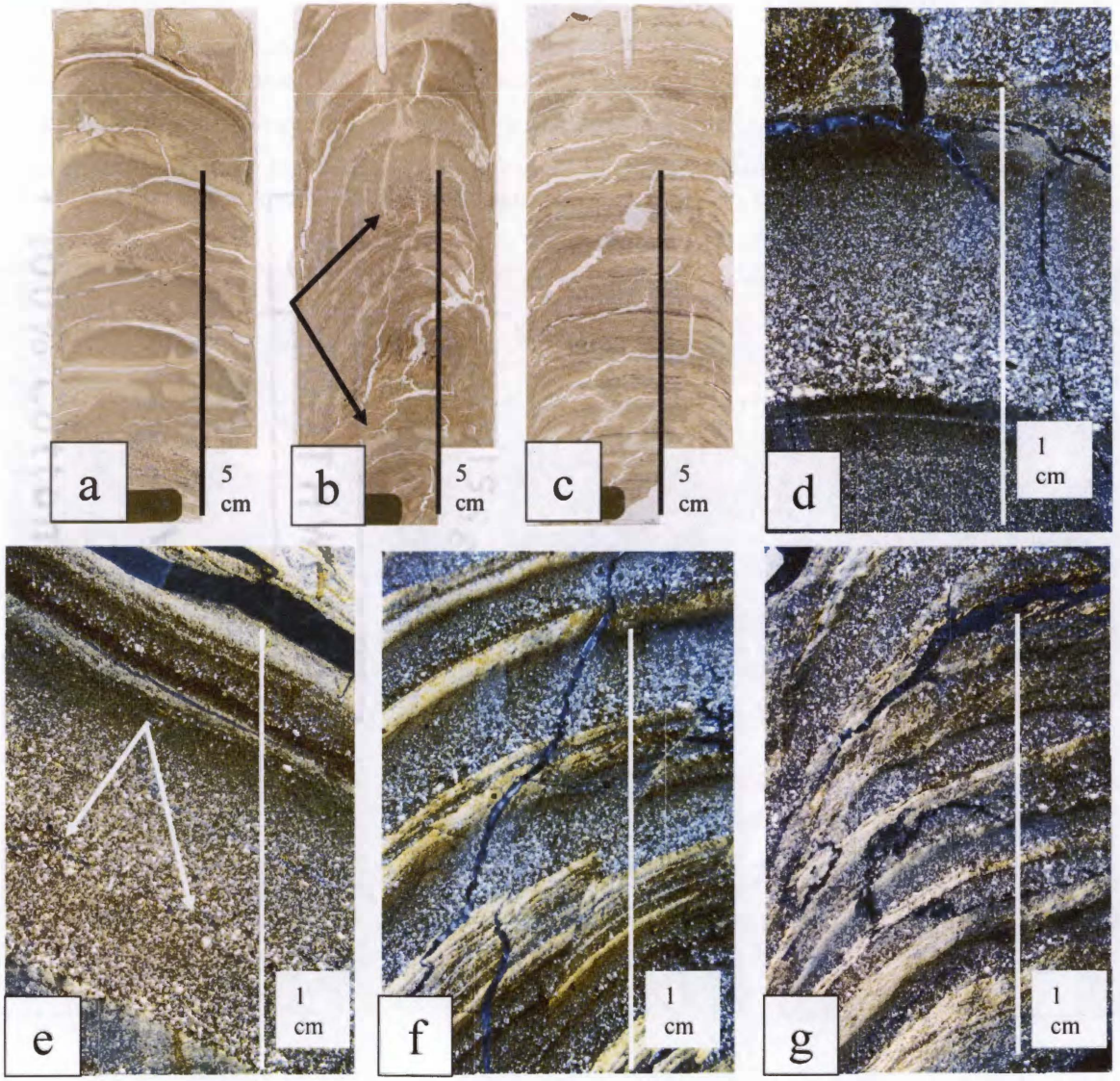

Fig. 9. Petrography of Graded Facies: 9(a-c). Thin-sections for *graded facies* at elevations of 496m, 498.5m, and 500m, respectively.

9(a). An example of the thick-graded beds characterized by sharp upper contacts that represent unconformities in deposition.

9(b). Sediments with thin-mixed depositional pattern (between arrows). Above and below are thick graded beds; notice the presence of two discrete depositional patterns.

9(c). Example of the thin-mixed depositional pattern, characterized by sequences of thin graded beds and mixed non-graded sediment.

9(d). A thick, individual graded bed. Long sequences of these beds characterize the graded facies.

9(e). An interrupted graded bed; the white arrows indicate an interruptive coarse layer.

9(f), (g). Thin-graded beds (f) and the thin/mixed depositional pattern (g) that characterize the transition from the *laminated facies* to the *graded facies*.

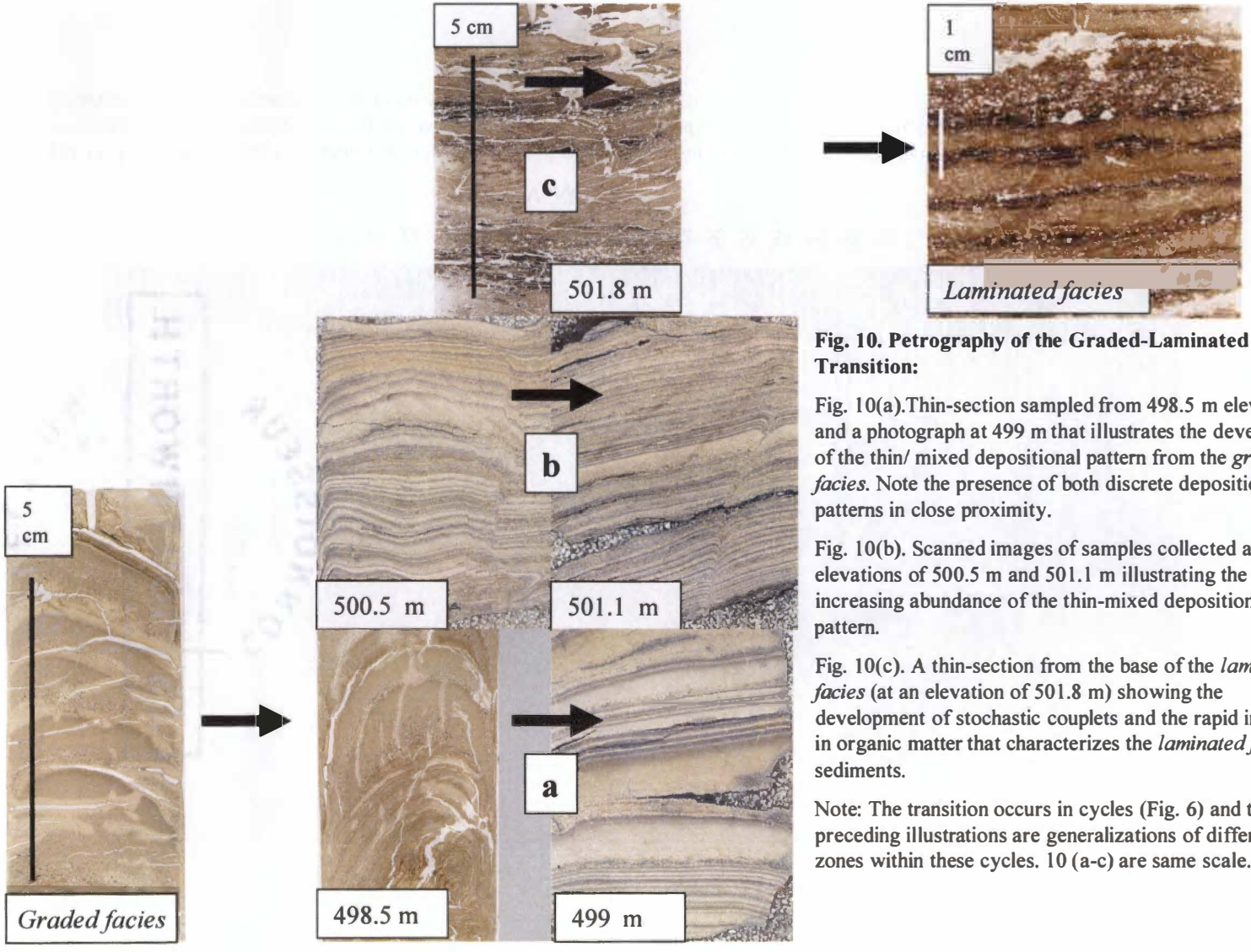

Fig. 10. Petrography of the Graded-Laminated Facies Transition:

Fig. 10(a).Thin-section sampled from 498.5 m elevation and a photograph at 499 m that illustrates the development of the thin/ mixed depositional pattern from the *graded facies*. Note the presence of both discrete depositional patterns in close proximity.

Fig. 10(b). Scanned images of samples collected at elevations of 500.5 m and 501.1 m illustrating the increasing abundance of the thin-mixed depositional pattern.

Fig. 10(c). A thin-section from the base of the *laminated facies* (at an elevation of 501.8 m) showing the development of stochastic couplets and the rapid increase in organic matter that characterizes the *laminated facies* sediments.

Note: The transition occurs in cycles (Fig. 6) and the preceding illustrations are generalizations of different zones within these cycles. 10 (a-c) are same scale.

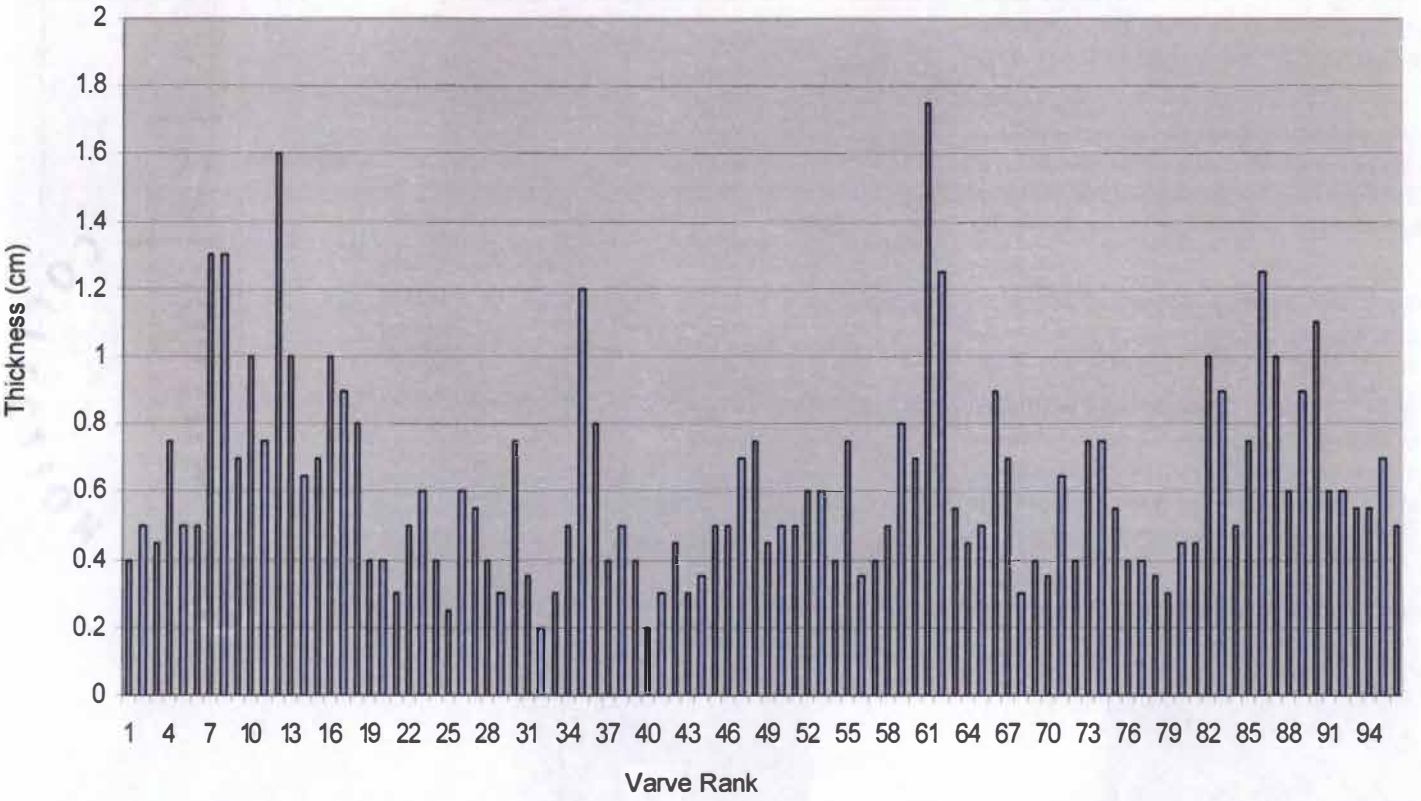

Fig.11. Varve Thickness vs. Rank: Individual varve thickness was measured from a series of 97 continuous couplets within the *laminated facies*. Spectral analysis of the data produced significant periodicity at a period of 5 couplets (Fig. 19). The oscillating thickness of the varves could be seen in the field.

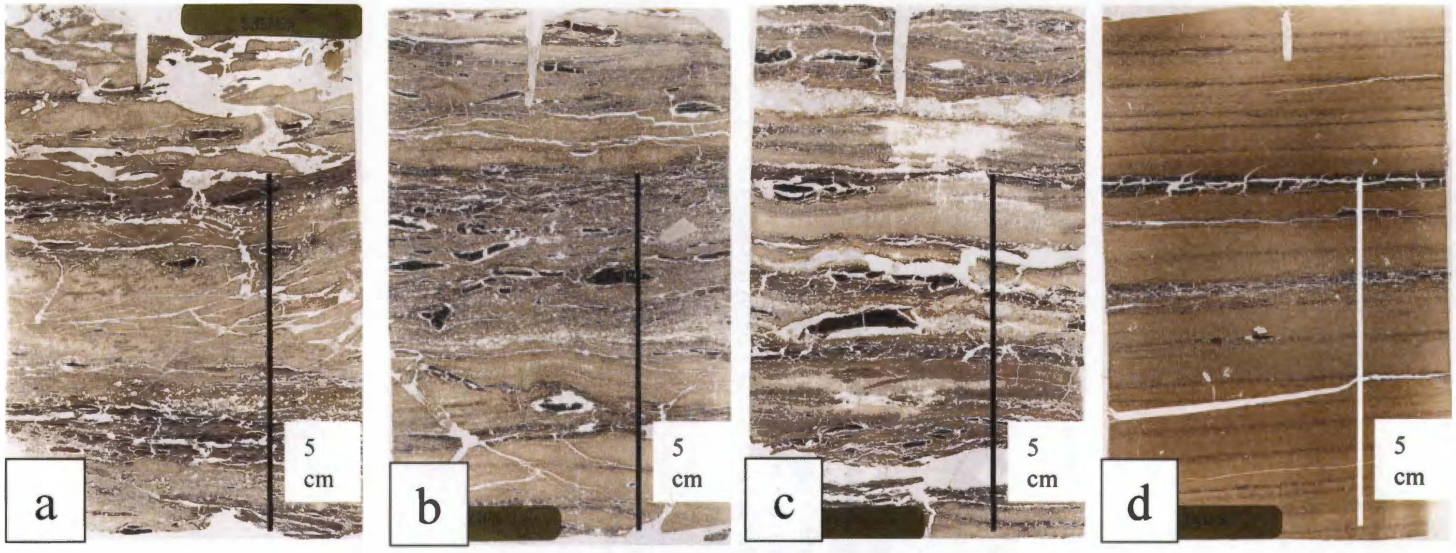

Fig. 12. Petrography of Laminated Facies:

12(a). Thin-section from an elevation of 501.8 m at the base of the *laminated facies* illustrating the stochastic depositional pattern.

12(b). Thin-section from an elevation of 502.5 m. Note: the thick (A) and (B) laminae that correlate to the return to stochastic deposition.

12(c). Thin-section from an elevation of 504.5 m. This thin-section indicates that the sediments could return to a stochastic depositional pattern at any elevation. Data for periodicity could not be recorded from this interval.

12(d). The most distinctly laminated sediments were destroyed by road-construction crews. This thin-section was made from the upper-most center portion of the site, but the exact elevation is unknown.

12(e). More typical of the *laminated facies* depositional pattern with distinct (A) and (B) laminae of variable thickness.

Fig. 13. Gray Fossil Site Grain Diversity: Assemblage of grains preserved within the GFS sediments.

Fig.13(a). Reworked soil aggregates in plain light (left) and cross-polarized light (right); 10x magnification. These grains were derived from a local paleosol forming at time of deposition. These rip-up grains occur exclusively within the (A) laminae in the *laminated facies,* suggesting that the landscape was eroding during the high-energy season.

Fig. 13(b). Monocrystalline quartz grains in plain light; 5x magnification. Some of the quartz grains at the center are pitted, with resorption rims. The presence of these elongate pits indicates that the quartz are derived from a volcanic origin. The closest possible source of these grains is >50 km away to the northeast (Smith, 2003).

Fig.13(c). Metamorphic polycrystalline quartz grains with elongated sub-grains. Cross-polarized light; 10x magnification.

Fig. 13(d). Chert clast derived from the local Knox Group dolostone in cross-polarized light; 5x magnification. Note the detrital carbonate around the large chert clast.

Fig. 13(e). Angular sucrosic dolostone clast in cross-polarized light at 1.5x magnification. This grain was derived from weathering of the local bedrock.

Fig. 13(f). Pyrite framboids in plain light; 10x magnification. The presence of pyrite within the GFS, as well as the preservation of the original sedimentological fabric without evidence of bioturbation, likely indicates that the GFS basin remained anoxic or poorly oxygenated.

Fig. 13(g). Siderite layers in plain light; 5x magnification. These layers are typically normally graded by size, but can also be mixed. Siderite can precipitate in saturated soils or when a solution containing Fe^{2+} and HCO_3^- evaporates or becomes alkaline.

a
1 mm
b
1 mm
c
1 mm
d
1 mm
e
1 cm
f
1 mm
g
1 mm

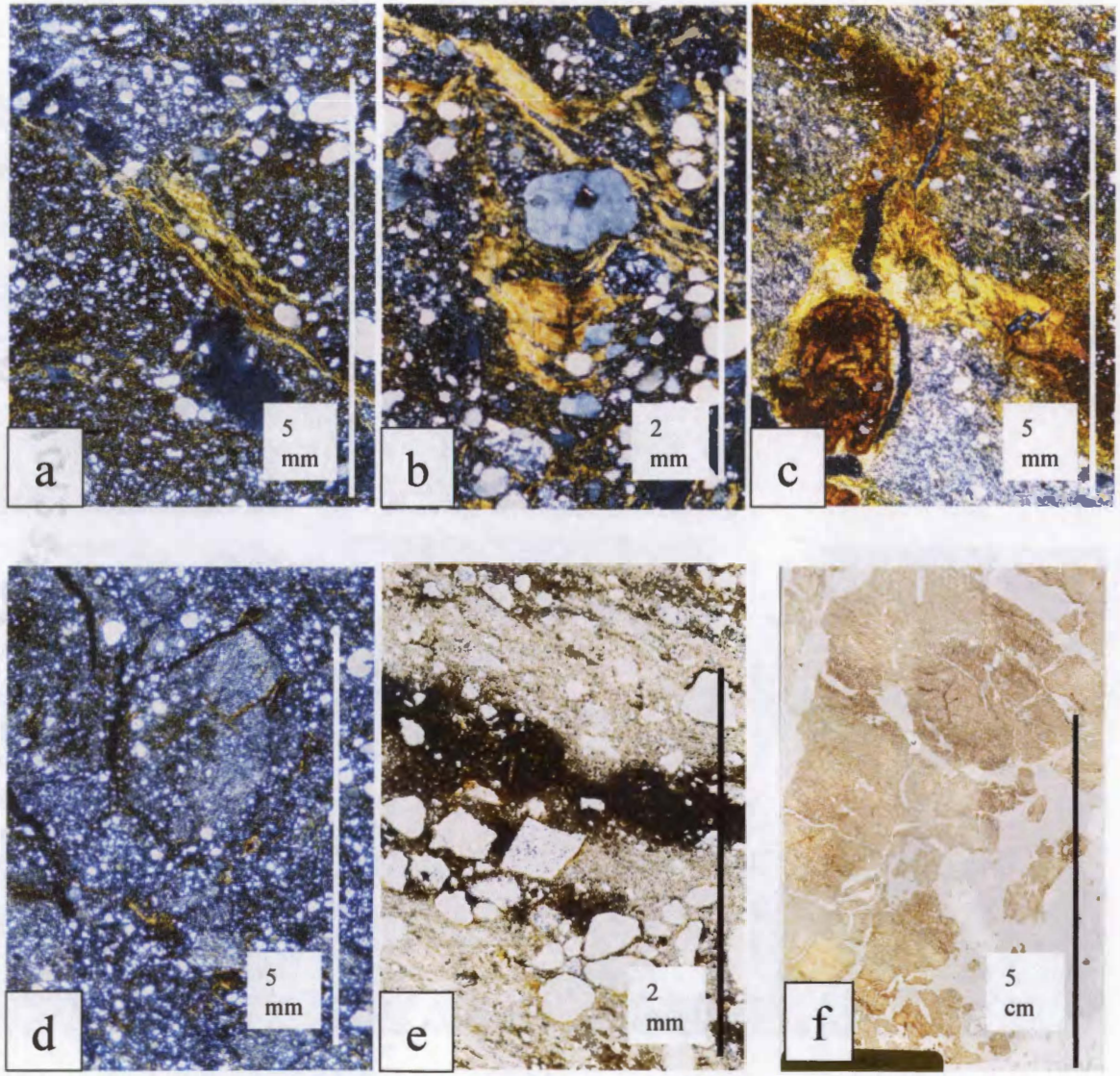

Fig. 14. Petrography of paleosol: Evidence of pedogenesis within the upper portion of the *laminated facies.*

Fig. 14(a). Note illuviated, birefringent clay in a root trace; Cross-polarized light.

Fig. 14(b). Illuviated, birefringent clay with a meniscate structure. Cross-polarized light.

Fig. 14(c). Birefringent clay without meniscate structure.

Fig. 14(d). Well-developed angular/ sub-angular peds; cross polarized light.

Fig. 14(e). Pedogenic iron manganese; plain light.

Fig. 14(f). Thin-section from the paleosol at an elevation of 504.8 m. The features noted in (a-e) are consistent with an Alfisol soil order that forms beneath forest environments and takes several thousand years to develop (Birkeland, 1999).

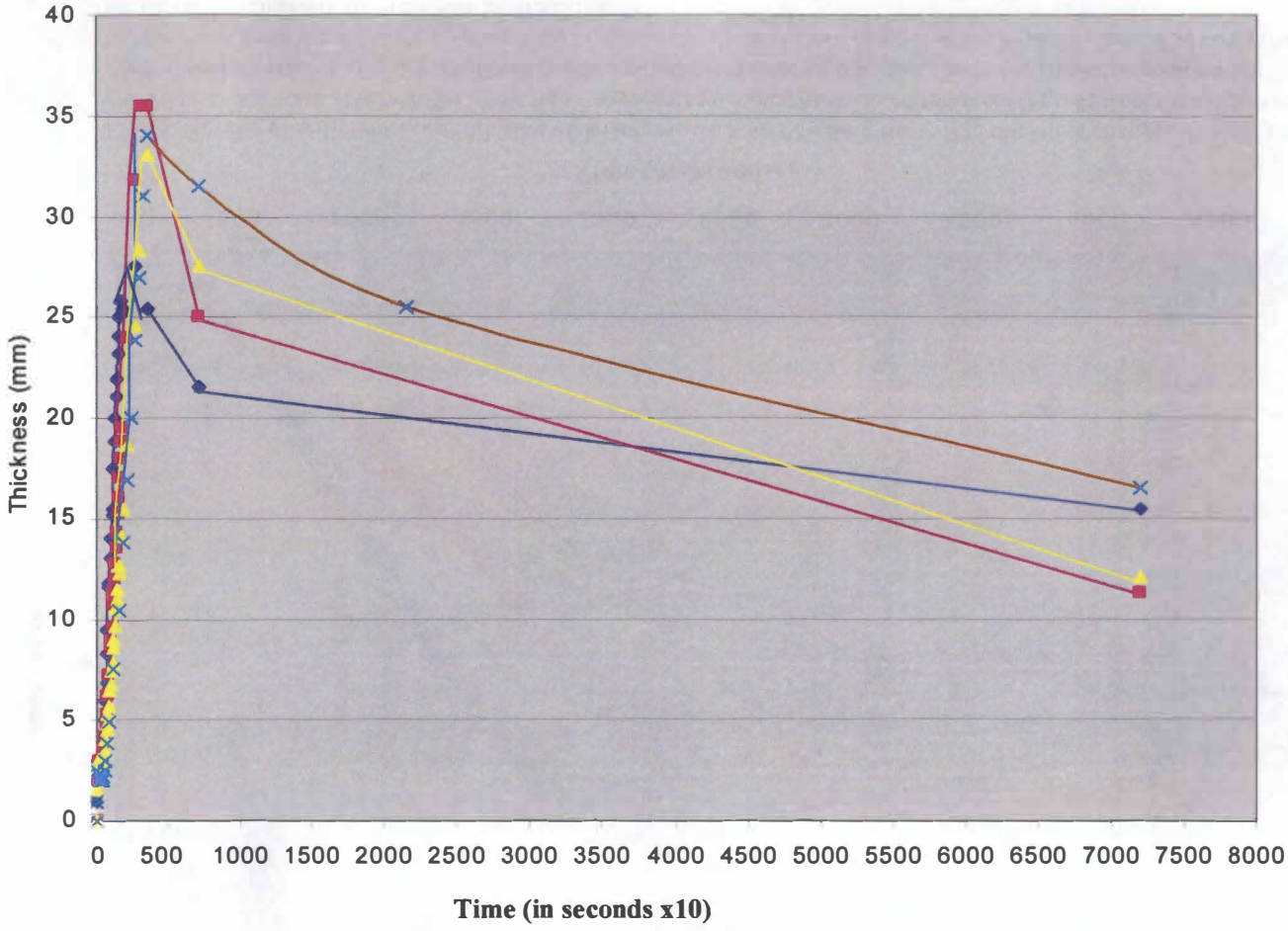

Fig.15. Results of sediment accumulation experiment, 21 hours settling time: Bed thickness changes through time for normally graded beds that were achieved by allowing disaggregated distinctly laminated sediment (Fig. 8) from the GFS to settle 1m in a vertical settling column (Fig. 7). Note the consistency within the four experiments and that the maximum thickness of each bed was achieved between 3,000-4,000 seconds (about one-hour). After that the beds continued to settle over the next 72,000 seconds (20 hours).

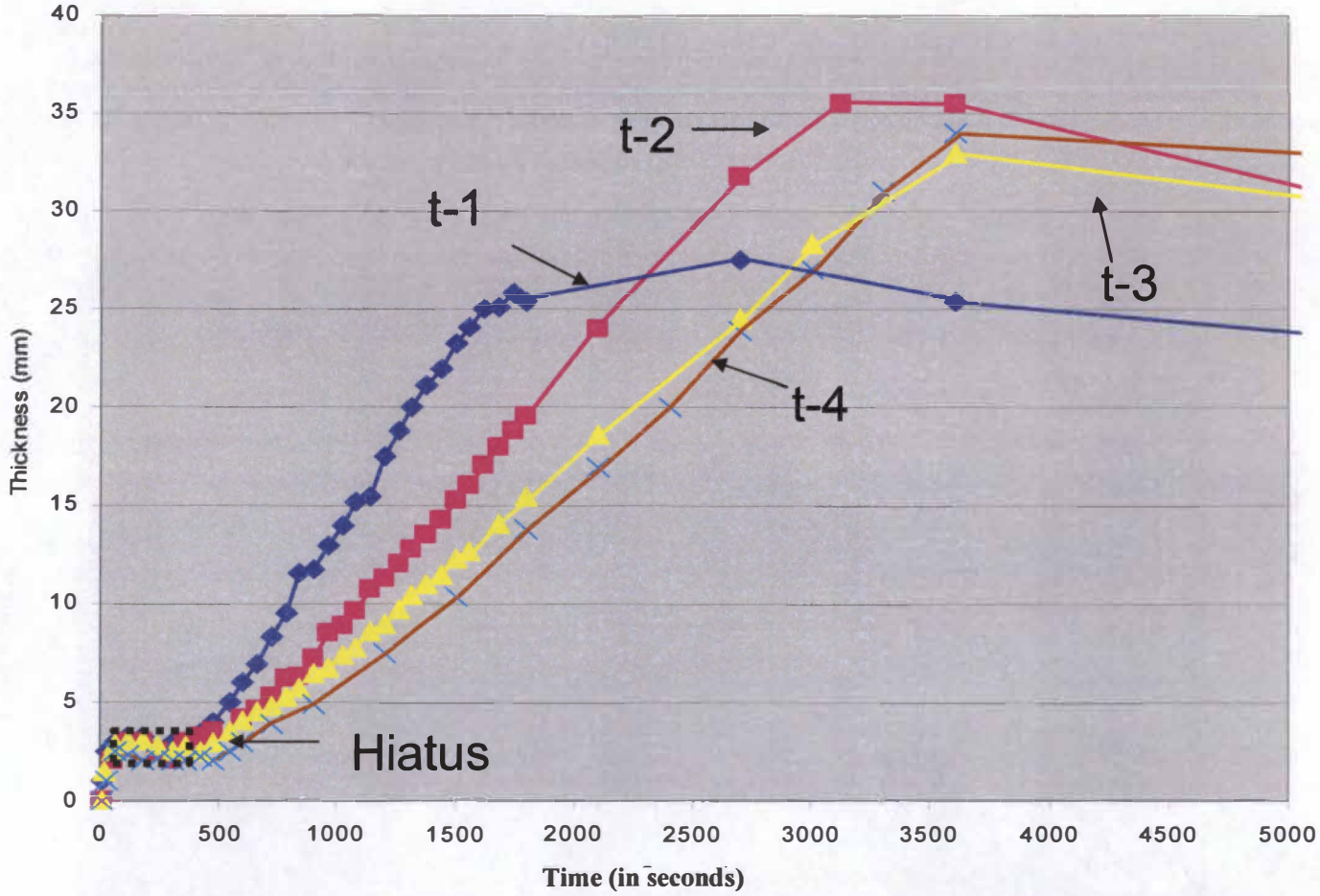

Fig.16. Results of sediment accumulation experiment, 1.4 hours settling time: Bed thickness changes through time for normally graded beds that were generated by allowing disaggregated distinctly laminated sediment (Fig. 8) from the GFS to settle 1m in a vertical settling column (Fig. 7). Note the hiatus separating the coarse component from the silty-clay component; the presence of this hiatus results from the difference between the settling velocity of the two distinct suites of grain sizes. The coarse suite of particles are derived exclusively from the (A) laminae (Fig. 8c).

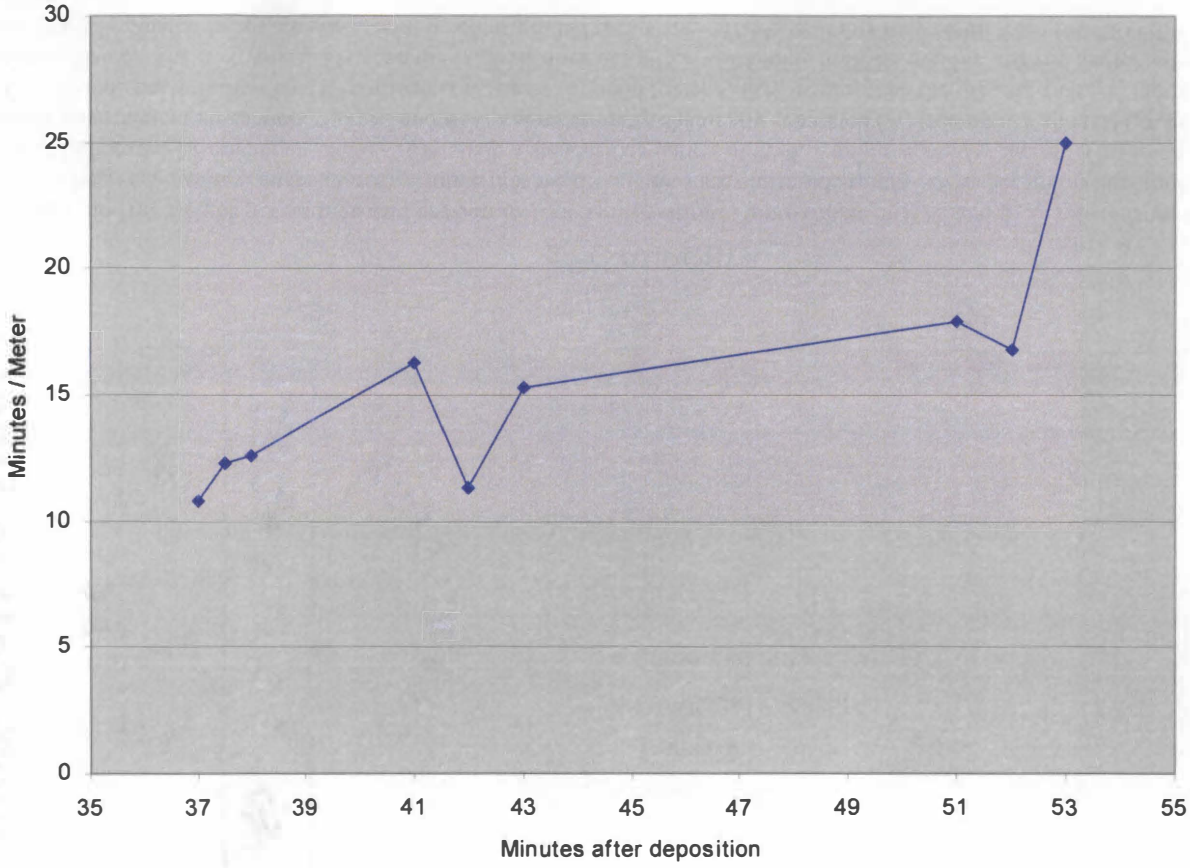

Fig.17. Results of sediment accumulation experiment, estimated clay settling velocity: Settling rate of individual clay flocculants during 3 cm settling at different times. Time is measured in the amount of time after the initial insertion of the sediments into the settling column. This trend was used to calculate an estimated settling velocity for the GFS clay particle sizes.

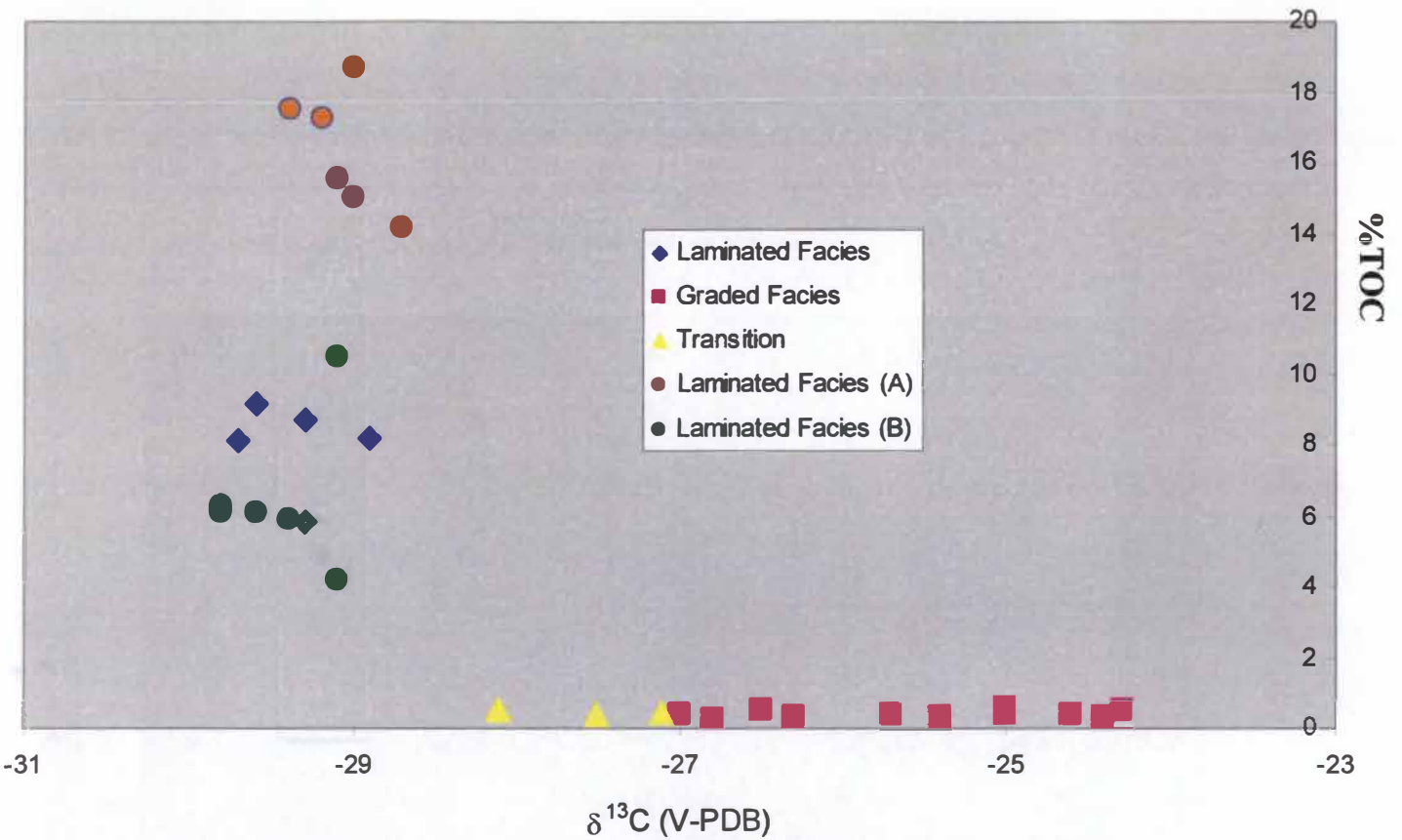

Fig.18. Organic matter weight percentage and carbon isotope composition: Approximate %TOC and d^{13}C values from the *laminated facies* (blue diamonds) and the *graded facies* (pink squares). Notice that the d^{13}C values are clustered around –29‰ per mil in the *laminated facies,* with a standard deviation of 0.29 but range from about –24 to –26‰, with a standard deviation of 0.98, within the *graded facies.* This trend may result from change from drier to wetter environment up-section. %TOC and d^{13}C values from mechanically separated (A) (red circle) and (B) (green circle) laminae from the *laminated facies* indicate the silty-clay (B) laminae consistently contain lower %TOC values than the organic-rich (A) laminae; thus the (A) and (B) laminae were isolated. The d^{13}C values between the laminae does not differ which may indicate that the organic matter source was constant. Note that d^{13}C values in the laminated facies are consistent, whereas graded facies are variable, and this may result from low %TOC or to variable sources of the organic matter.

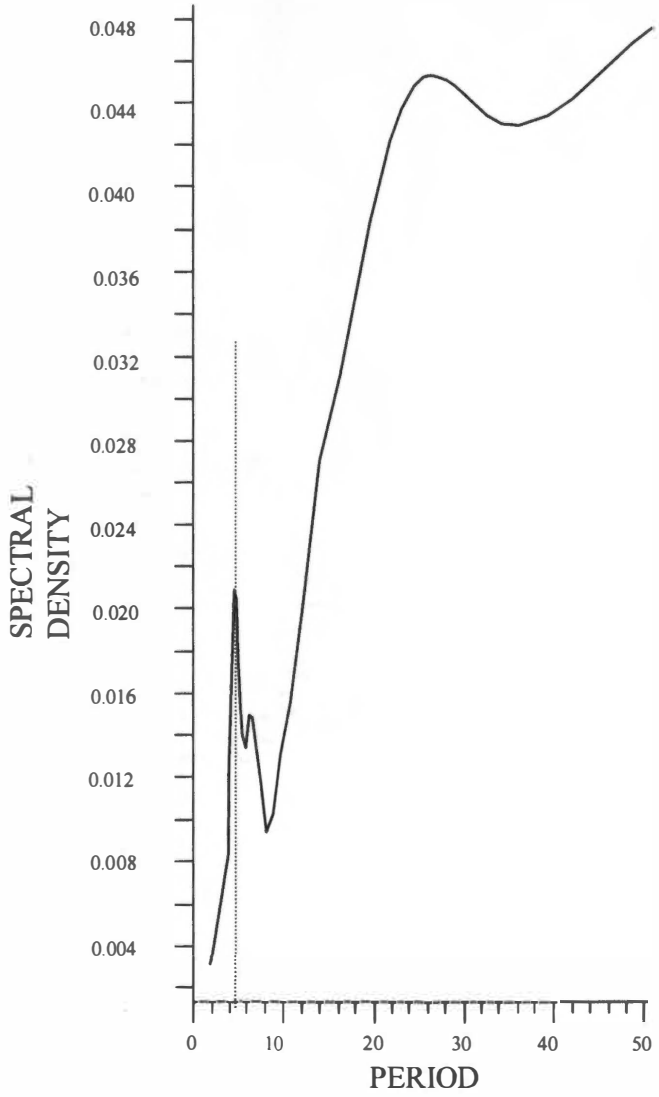

Fig. 19. 5-year periodicity: Periodogram calculated for the distinctly laminated lacustrine sediments. The Fisher's Kappa value is 7.42, which establishes the largest peak, at a period of about 5, is not white noise. Spectral density is a function that quantifies the variance between adjacent points in a continuous series of data. In this case the variance was the thickness of adjacent annual varve couplets (Fig. 11). Similar 5-year periodicity from the Eocene age Green River Formation has been interpreted to result from ENSO control on annual sediment thickness (Ripepe et al., 1991); a similar interpretation is inferred for the GFS sediments.

Fig. 20. Conceptualized GFS Geomorphic and Stratigraphic Development : A conceptual model of the progressive geomorphic and stratigraphic development of the GFS. The conceptual model is based on the geomorphic development of sinkhole lake in north-central FL (Kidinger, 1996). The stratigraphy within the GFS (Fig. 6) is consistent with a conceptual model that includes:

Fig.20.(a). The Active or Collapse Sinkhole Phase- the initial stage of sinkhole development in which surface water is transferred into an underlying aquifier.

Fig.20.(b). Transitional Phase- partially sediment filled, sediment may be periodically flushed down the sinkhole collapse, thus causing reactivation of sinkhole Active Phase (may happen numerous times). As the lake develops, Knox residuum forms at the surface of the site.

Fig.20.(c). Base Level Phase- GFS has been plugged with sediment and is now a buried sinkhole lacustrine environment. Like all lakes the GFS is an ephemeral feature of the landscape and constantly fills with sediment.

Fig.20.(d). Subaerial Phase- GFS is exposed to the atmosphere and soil development begins. Water table flctuations may reactivate the Base level Phase and additional lacustrine sediment may be deposited during periods high water levels.

Fig.20.(e). A combination of chert-rich alluvium and colluvium regolith are deposited and armor the site (Clark, 2001, Smith, 2003).

Fig.20.(f). In May of 2000 the site is discovered when the sediments are exposed by heavy machinery extending a local road.

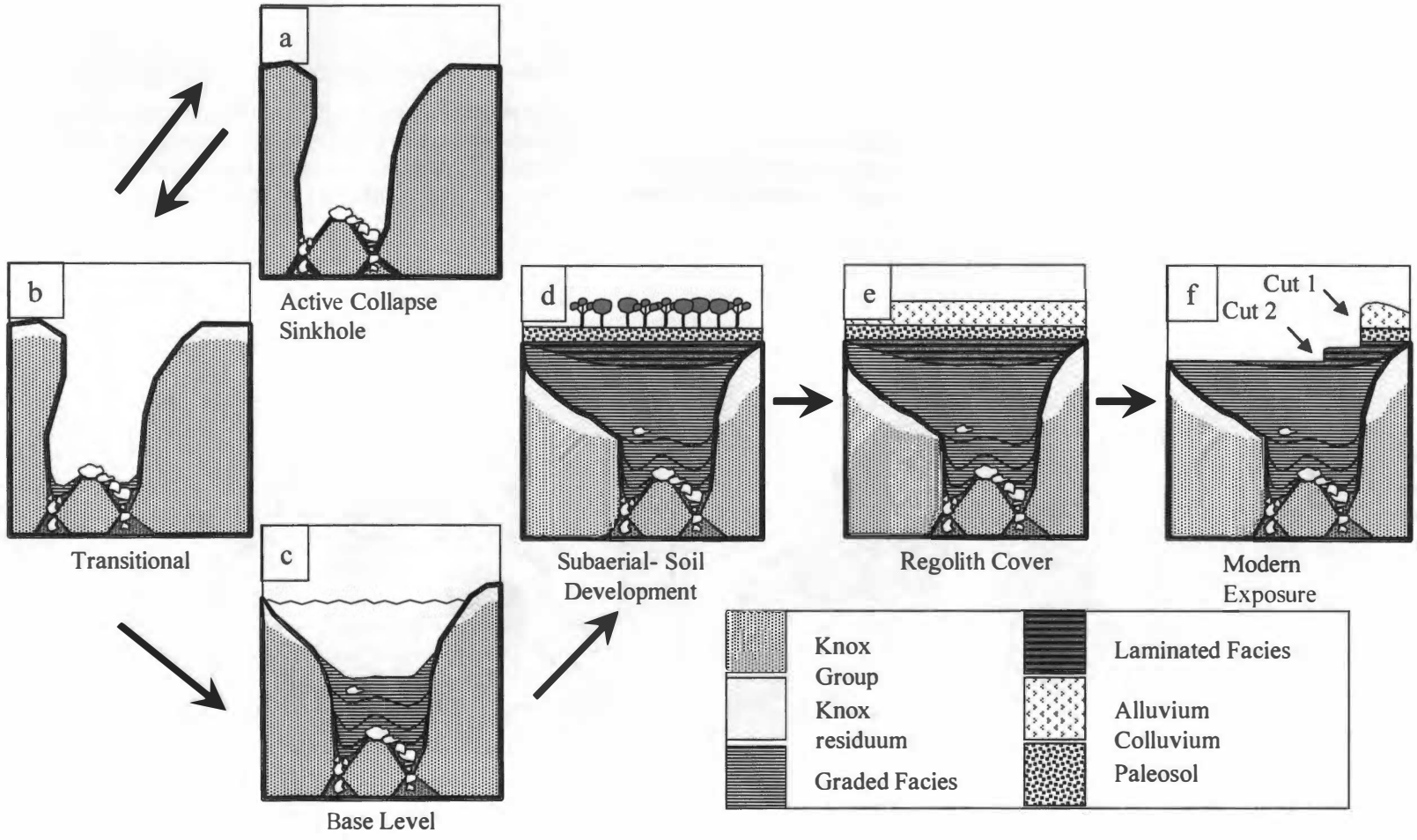
a
Active Collapse
Sinkhole
b
Transitional
c
Base Level
d
Subaerial- Soil
Development
e
Regolith Cover
f
Cut 1
Cut 2
Modern
Exposure
Knox
Group
Knox
residuum
Graded Facies
Laminated Facies
Alluvium
Colluvium
Paleosol

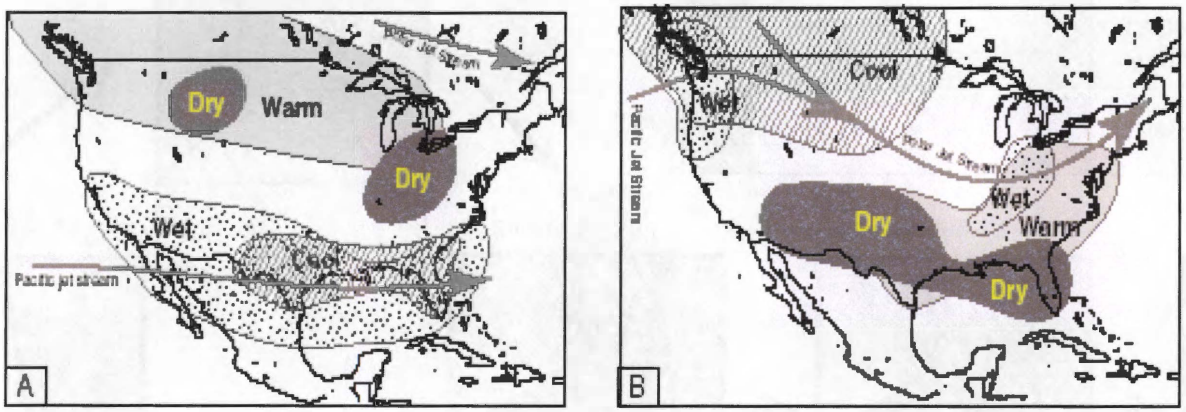

Fig. 21. Modern El Niño and La Niña cycles affect moisture delivery: The modern El Niño (A) and La Niña (B) cycle causes increased and decreased amounts of moisture in notheastern TN that may be responsible for the cyclic variation of couplet thickness within the *laminated facies*. Modern ENSO effect does not operate on a 5-year periodicity, but it is possible that during the latest Miocene-earliest Pliocene, the El Niño/ La Niña phenomenon was related to a different situation that caused a 5-year cycle of wet and dry climate.

This figure is modified from http://www.cpc.ncep.noaa.gov.

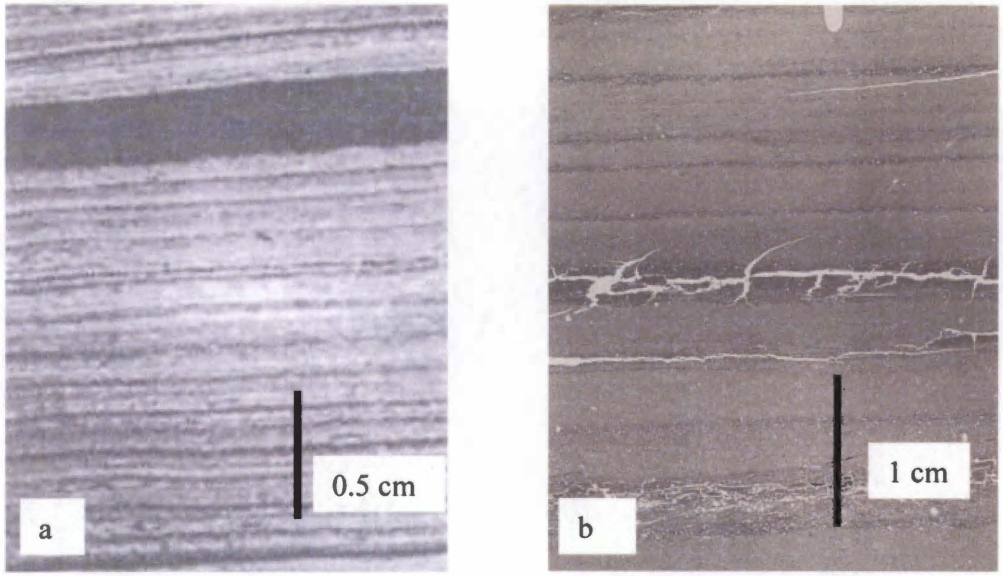

Modern Indian Monsoon from the Arabian sea

Early Pliocene GFS distinctly laminated facies

Fig. 22. Comparison of depositional patterns formed in response to modern Indian monsoon, and Late Hemphillian Gray Fossil Site:

Although each of the three sites has a different type of basin the general deposition pattern of both couplet components between the Arabian Sea and the GFS sediments are terrigenous and relate to high-energy season deposits, possibly indicating that the depositional patterns are derived from a similar mechanism (Table 6). There does not appear to be a clear modern analogue to the GFS sediments published in the literature.

(a). Modern Arabian Sea annual varves sediments from (Rad et al., 1999).

(b). Gray Fossil Site laminated sediments that are interpreted to represent annual varves.

Scale in (a) and (b) are estimations.

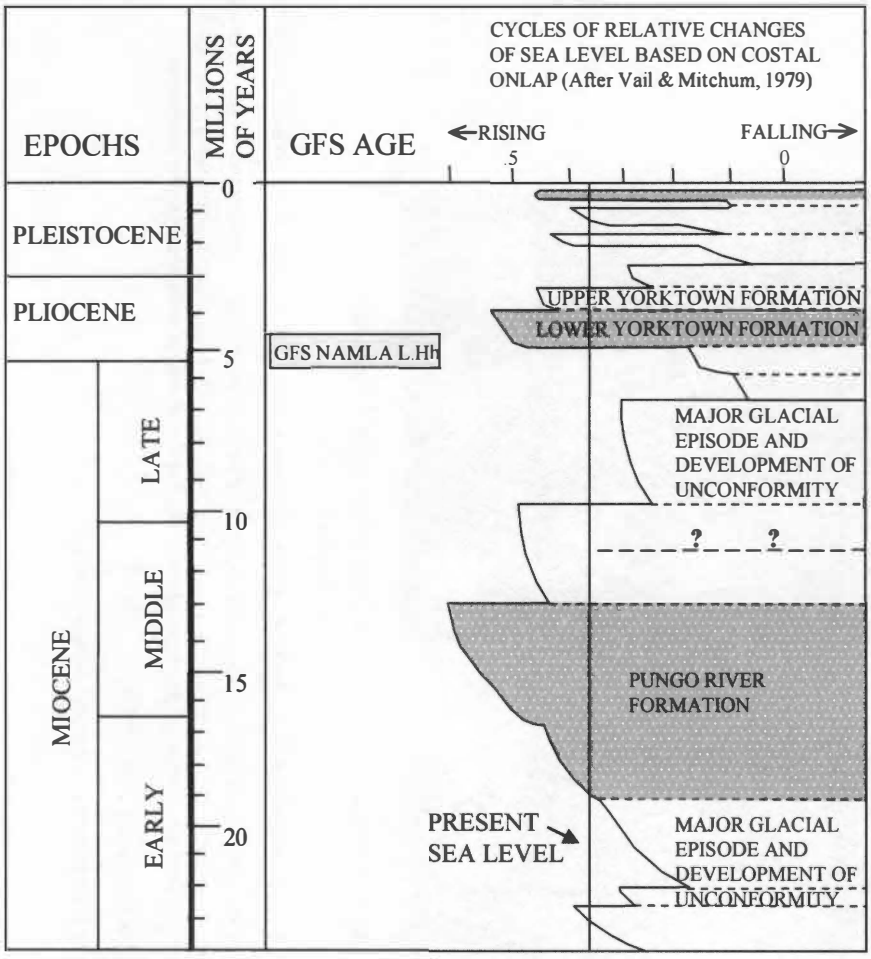

Fig.23. Atlantic Ocean Upwelling: Neogene stratigraphic section for the North Carolina continental margin (modified from Riggs, 1988) superimposed upon the second- and third-order coastal onlap curves of Vail and Mitchum (1979). Stratigraphic units containing anomalous concentrations of phosphate from upwelling are stippled. The Gray Fossil Site (GFS) is a Late Hemphillian (5.5 to 4.5 Ma) terrestrial fossil site at approximately the same latitude as the episode of Early Pliocene upwelling (about 4 to 5 Ma) in North Carolina. This figure indicates that the age range of deposition of laminated sediments at the GFS is potentially contemporaneous with Early Pliocene phosphogenesis in the Lower Yorktown Formation.

VITA:

Aaron Shunk was born in Muncie, Indiana on November 9, 1976. His immediate family includes his mother, Anna Shunk, his father, John Shunk, and one brother, Adam Shunk. Aaron attended high school at Delta High School and undergraduate at Ball State University, where he received a B.S. in Biology/Education. While studying at Ball State, he took interest in biological evolution and geologic time; two concepts he was denied in his upbringing. He attended graduate school at the University of Tennessee to pursue his interests in research in hopes of getting published.

After receiving an M.S. in Geology from the University of Tennessee, Aaron intends to pursue employment in either the petroleum or environmental industries.